PHYSICAL REVIEW B **75**, 035210 (2007)

Self- and foreign-atom diffusion in semiconductor isotope heterostructures. I. Continuum theoretical calculations

H. Bracht*

Institute of Materials Physics, University of Münster, D-48149 Münster, Germany

(Received 11 August 2006; published 17 January 2007)

Dopant diffusion experiments in semiconductors yield the mobility of the element of interest and information about the possible mechanisms of atomic diffusion. In many cases the diffusion is described on the basis of Fick's law of diffusion, but this treatment is often too simple. In this paper, dopant diffusion in semiconductors is treated systematically on the basis of diffusion-reaction equations. Predictions on the shape of dopant-diffusion profiles that develop under specific experimental conditions are derived. It is illustrated that the charge states of the point defects involved in the diffusion process strongly affect the shape of the dopant profile under electronically extrinsic conditions. The relation between the shape of the dopant profile and the underlying mechanism of atomic diffusion, and between the apparent dopant diffusion coefficient and the point defect mediating the diffusion process is explained. With the advance in epitaxial deposition techniques and the availability of isotopically enriched elements, semiconductor isotope heterostructures can be grown, which are highly appropriate for studying the impact of dopant diffusion on self-diffusion. The modeling of the simultaneous diffusion of self- and dopant atoms in semiconductor isotope heterostructures is described and the advances resulting from this new diffusion approach compared to conventional diffusion studies that treat self- and dopant diffusion separately, are highlighted. This paper aims to serve as a useful guide to understand and accurately model the diffusion of dopants and their impact on self-diffusion in semiconductors.

DOI: 10.1103/PhysRevB.75.035210 PACS number(s): 61.72.Ji, 66.30.Dn, 66.30.Hs, 66.30.Jt

I. INTRODUCTION

The understanding of defect reactions and dopant diffusion in semiconductors is crucial for controlling the distribution of dopants during the fabrication of electronic devices. In particular, this is important to meet the requirements for the continuing decrease of the lateral and vertical dimensions of semiconductor devices. Numerous diffusion experiments and spectroscopic studies have been conducted over the past few decades to determine the mechanisms of atomic-mass transport of self- and foreign atoms in elemental and compound semiconductors and the properties of point defects such as their structure, charge states, and formation and migration energies.[1–3] The advances in the understanding of atomic-transport processes and defect reactions in semiconductors has contributed to the remarkable increase of computer speed and capacity over the last two decades. On the other hand, the higher computer power gives rise to more reliable and predictive theoretical calculations of the properties of point defects in semiconductors and hence also expedites their own technological evolution. First-principle calculations based on density functional theory,[4–15] tight-binding molecular dynamics (TBMD) simulations,[16–19] and molecular dynamic (MD) calculations based on empirical interatomic potentials[20–23] provide valuable information about formation energies and charge states of thermodynamically stable defects and about diffusion paths and migration energies. However these calculations are still restricted to limited supercells and short times and hence provide a more microscopic view on the defect kinetics in a solid. On the other hand, Monte Carlo (MC) calculations represent a statistical approach, which can describe diffusion and reaction processes of point defects for longer times (see e.g., Ref. 24). An even more macroscopic approach of modeling the diffusion and reaction of point defects are continuum-theoretical (CT) calculations based on differential equations. Compared to MC calculations the continuum theory provides a robust and fast approach and even enables fits to experimental profiles that are hardly possible with the other methods. Within the CT approach model parameters can be directly related to the experimental profiles and a straightforward interpretation of the diffusion process and the apparent diffusion coefficients can be given.[25–38] Although the approach is more macroscopic compared to *ab initio* and MD simulations, the CT approach can provide information about the nature of the point defects, their charge states, and migration and formation enthalpies. A comparison of these results with *ab initio* and MD simulations yields information about the most likely microscopic structure and migration path of the defect.

It is noteworthy that besides diffusion studies no other experimental approach is available for studying the properties of point defects in solids at temperatures relevant for device process technology. An exception is the positron annihilation spectroscopy (PAS). However this method is limited to the investigation of vacancylike defects. The significance of diffusion studies for evaluating the properties of point defects is often underestimated.

In this paper general aspects of dopant diffusion in semiconductors are treated to explain the occurrence of characteristic dopant profiles. Although most of the diffusion models have been already described in some review papers (see e.g., Refs. 25, 26, and 28) a comprehensive treatment that also explains the interference between self- and dopant diffusion is lacking. The most relevant mechanisms of diffusion in semiconductors are discussed in Sec. II, taking into account that the defects involved can exist in various charge

 ©2007 The American Physical Society

states (see Sec. II A). Since the impact of point-defect charges on the diffusion of an element has neither been considered in general nor treated in detail, Secs. II B and II C summarize a continuum theoretical description of diffusion in semiconductors, which takes into account the diffusion of a charged defect X in the presence of an electric field. Representative for all indirect diffusion mechanisms, the mathematical description of the vacancy and dissociative diffusion mechanisms is treated in Secs. II D and II E, respectively. It is demonstrated that the shape of the diffusion profile of a mainly substitutional dissolved element A_s depends on the diffusion mechanism and the specific charge states of the point defects involved. The understanding of this dependency is helpful to directly obtain from the shape of the experimental dopant profile information about the mechanism that can mediate dopant diffusion and those mechanisms that can be excluded. Finally, a general CT description of the simultaneous diffusion of self- and foreign atoms is presented in Sec. III. First, the impact of doping on the formation of point defects is treated in Sec. III A. Then, a general equation for self-diffusion is formulated in Sec. III B that considers local concentrations of point defects and possible contributions of dopant-defect pairs to self-diffusion.

The CT description of the impact of dopant diffusion on self-diffusion is highly appropriate for modeling the interference of self- and foreign atoms in isotopically enriched semiconductors. Numerical simulations on the simultaneous diffusion are shown in Sec. III C. The simulations are representative for modeling the diffusion of boron, arsenic, or phosphorus in silicon isotope multilayer structures. The results of these experiments are the subject of Part II following this paper.

II. MECHANISMS OF DIFFUSION IN SEMICONDUCTORS

A. Direct and indirect mechanisms

The mechanisms of diffusion in semiconductors are in general divided in direct and indirect mechanisms. Figure 1 illustrates various diffusion mechanisms of a foreign atom A in an elemental semiconductor or in the sublattice of a binary compound. The diffusion of mainly interstitially dissolved foreign atoms with charge state q, A_i^q, proceeds via interstitial lattice sites. No native point defects need to be involved in this direct interstitial mechanism [see Fig. 1(a)]. A direct diffusion of atoms on substitutional sites with charge state m, A_s^m, can occur via a direct exchange with adjacent matrix atoms or a ring mechanism. So far no convincing experimental evidence has been found for this direct mechanism indicating that the diffusion of A_s^m via indirect mechanisms is in general energetically more favorable.

Various indirect diffusion mechanisms are illustrated in Fig. 1(b), which involve native-point defects like vacancies V^k and self-interstitials I^u. These mechanisms are described by the following reactions:

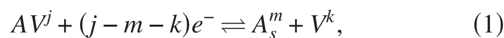

$$AV^j + (j-m-k)e^- \rightleftharpoons A_s^m + V^k, \qquad (1)$$

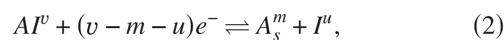

$$AI^v + (v-m-u)e^- \rightleftharpoons A_s^m + I^u, \qquad (2)$$

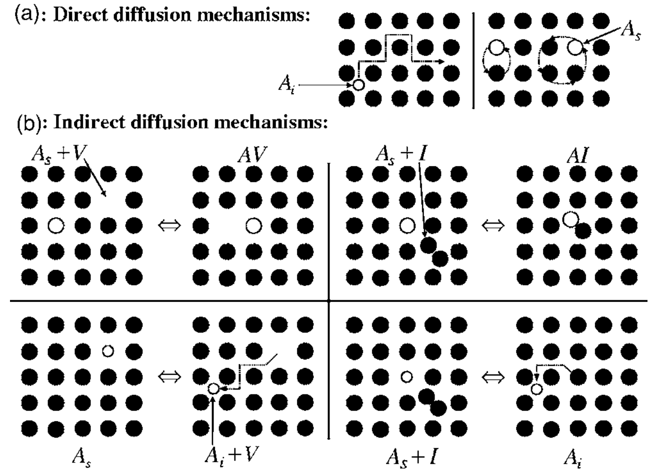

FIG. 1. Schematic two-dimensional representation of (a) direct and (b) indirect diffusion mechanisms of an element A in a solid. A_i, A_s, V, and I denote the interstitially and substitutionally dissolved foreign atoms, the vacancy, and self-interstitial, respectively. AV and AI are defect pairs of the corresponding defects. For simplicity the subscripts indicating the charge states of the defects were omitted.

$$A_i^q + (q-m-u)e^- \rightleftharpoons A_s^m + I^u, \qquad (3)$$

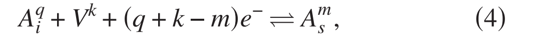

$$A_i^q + V^k + (q+k-m)e^- \rightleftharpoons A_s^m, \qquad (4)$$

with the charge states $j,k,m,q,u,v \in \{0,\pm 1,\pm 2,\ldots\}$ and the electrons e^-. Reactions (1) and (2) represent the vacancy and interstitialcy mechanisms, respectively. The third and fourth reactions are the kick-out and the dissociative (or Frank-Turnbull) mechanism, respectively. They describe the diffusion behavior of hybrid elements, which are mainly dissolved on substitutional sites but move as interstitial defects A_i^q as illustrated in Fig. 1(b).

In addition to reactions (1)–(4) other reactions between point defects and defect pairs can be considered. Beside the so-called Frenkel-pair reaction,

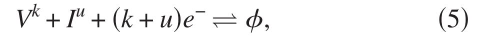

$$V^k + I^u + (k+u)e^- \rightleftharpoons \phi, \qquad (5)$$

which describes the annihilation (formation) of V^k and I^u into (from) self-atoms on regular lattice sites, the reactions

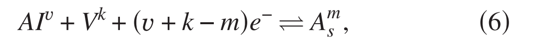

$$AI^v + V^k + (v+k-m)e^- \rightleftharpoons A_s^m, \qquad (6)$$

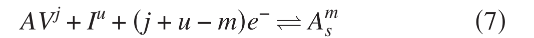

$$AV^j + I^u + (j+u-m)e^- \rightleftharpoons A_s^m \qquad (7)$$

describe the dopant-defect pair assisted recombination of V^k and I^u.

Generally, reactions (1)–(7) are fast processes compared to the time scale of diffusion, which typically amounts to several minutes up to several hours. For these conditions local equilibrium of the reactions is reached. Local equilibrium in the case of the kick-out reaction (3) and the dissociative reaction (4) is characterized by

$$\frac{C_{A_s^m} C_{I^u}}{C_{A_i^q} n^{(q-m-u)}} = \frac{C_{A_s^m}^{\mathrm{eq}} C_{I^u}^{\mathrm{eq}}}{C_{A_i^q}^{\mathrm{eq}} (n^{\mathrm{eq}})^{(q-m-u)}}, \qquad (8)$$

$$\frac{C_{A_s^m}}{C_{A_i^q} C_{V^k} n^{(q+k-m)}} = \frac{C_{A_s^m}^{\text{eq}}}{C_{A_i^q}^{\text{eq}} C_{V^k}^{\text{eq}} (n^{\text{eq}})^{(q+k-m)}}. \tag{9}$$

C_X (C_X^{eq}) represents the (thermal equilibrium) concentration of the defect X with $X \in \{A_i^q, A_s^m, I^u, V^k\}$. n (n^{eq}) denotes the (maximum) free-electron concentration. It is noted that local equilibrium does *not* imply that the concentrations of self-interstitials and vacancies equal their thermal equilibrium values $C_{I^u}^{\text{eq}}$ and $C_{V^k}^{\text{eq}}$; locally the concentration of the native defects can deviate from thermal equilibrium. Introducing defect and electron concentrations normalized to their thermal equilibrium values, $\tilde{C}_X = C_X / C_X^{\text{eq}}$ and $\tilde{n} = n/n^{\text{eq}}$, Eqs. (8) and (9) yield

$$\frac{\tilde{C}_{A_s^m} \tilde{C}_{I^u}}{\tilde{C}_{A_i^q} \tilde{n}^{(q-m-u)}} = \frac{\tilde{C}_{A_s^m}}{\tilde{C}_{A_i^q} \tilde{C}_{V^k} \tilde{n}^{(q+k-m)}}, \tag{10}$$

which simplifies to

$$\frac{1}{\tilde{C}_{V^k} \tilde{C}_{I^u} \tilde{n}^{(k+u)}} = 1. \tag{11}$$

Equation (11) expresses local equilibrium of the Frenkel-pair reaction (5) and shows that this equilibrium state is established when local equilibrium of the kick-out and dissociative reactions holds. On the other hand, under local equilibrium conditions experimental diffusion profiles, which are described on the basis of the kick-out and dissociative reactions can also be modeled on the basis of the kick-out and Frenkel-pair reactions or the dissociative and Frenkel-pair reactions. In this respect diffusion experiments for times when local equilibrium is established are not appropriate to identify the mechanisms of diffusion. This loss of unambiguousness also holds for other combinations of diffusion reactions. The three combinations of each two reactions from Eqs. (2), (5), and (6) all predict identical diffusion profiles for local equilibrium. Moreover, Eqs. (2) and (4) are mathematically equivalent to Eqs. (3) and (6), respectively. Accordingly, the three combinations of each two reactions from Eqs. (3)–(5) also lead to identical diffusion profiles to those from Eqs. (2), (5), and (6). This shows that dopant diffusion alone can hardly distinguish between A_i^q and AI^v. However, dopant diffusion in isotope heterostructures can, in principle, differentiate between interstitial foreign atoms and the dopant-defect pairs, because the pairs may also contribute to self-diffusion (see Sec. III B). Therefore, both A_i^q and AI^v are considered as possible mobile defects mediating dopant diffusion.

B. Phenomenological description of diffusion

The continuum theoretical treatment of mass transport in solids is based on Fick's law of diffusion. In one dimension the diffusion equation takes the generalized form

$$\frac{\partial C_X}{\partial t} + \frac{\partial}{\partial x} J_X = G_X, \tag{12}$$

where C_X and J_X, respectively, are the concentration and flux of a point defect $X \in \{A_i^q, A_s^m, I^u, V^k, AV^j, AI^v\}$ as a function of time t and position x. Possible reactions between X and other defects are taken into account by G_X. In the case where the flux is mainly determined by the diffusion of X, i.e.,

$$J_X = -D_X \frac{\partial C_X}{\partial x}, \tag{13}$$

the diffusion equation is given by

$$\frac{\partial C_X}{\partial t} - \frac{\partial}{\partial x}\left(D_X \frac{\partial C_X}{\partial x} \right) = G_X. \tag{14}$$

For the diffusion of an element A, which is mainly dissolved on interstitial sites and diffuses via the direct interstitial mechanism, we get $X = A_i^q$ and $D_A = D_{A_i^q}$. In this case no reaction takes place during diffusion, accordingly $G_X = 0$. If a constant concentration $C_{A_i^q}^{\text{eq}}$ is maintained at the surface, the solution of Eq. (14) is given by

$$C_{A_i^q} = C_{A_i^q}^{\text{eq}} \left[1 - \text{erf}\left(\frac{x}{2\sqrt{D_{A_i^q} t}} \right) \right], \tag{15}$$

with a concentration-independent diffusion coefficient $D_{A_i^q}$. This solution holds for the diffusion of mainly *interstitially* dissolved foreign atoms ($X = A_i^q$) such as hydrogen, lithium, and the 3d transition metals in silicon[1] provided that their diffusion is not affected by complex formation between the foreign atom and other defects. Fitting of the concentration profiles directly yields the interstitial diffusion coefficient $D_{A_i^q}$.

The diffusion of mainly substitutionally dissolved foreign atoms ($X = A_s^m$) often results in diffusion profiles, which deviate from Eq. (15) (see e.g., Ref. 1). The apparent diffusion coefficient D_A is a complex quantity, which depends on the diffusion coefficient of the point defect that controls the diffusion process and the equilibrium concentrations of other defects involved in the defect reaction (see below). Typical diffusion profiles of an indirectly diffusing element A that imply a concentration-dependent diffusion coefficient of the form of

$$D_A \propto (C_A)^r, \tag{16}$$

with $r \in \{-2, 0, 1, 2\}$ are shown in Fig. 2.

Generally, several mechanisms may contribute to the diffusion coefficient D_A of a mainly substitutionally dissolved element A. Taking into account all possible contributions, D_A is given by

$$D_A = D_A^{(1)} + D_A^{(2)} + D_A^{(3)} + D_A^{(4)} + D_A^{\text{ex}}. \tag{17}$$

$D_A^{(1)}$, $D_A^{(2)}$, $D_A^{(3)}$, and $D_A^{(4)}$ represent contributions due to the various indirect diffusion mechanisms given by reactions (1)–(4) and illustrated in Fig. 1. Each diffusion coefficient can be a complicated function of the concentration and dif-

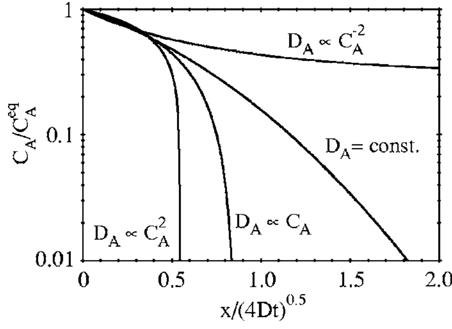

FIG. 2. Concentration profiles of an element A normalized by its equilibrium concentration C_A^{eq} versus the normalized penetration depth $x/\sqrt{4D_At}$. The profiles represent solutions of Eq. (14) with $G_A=0$ for different concentration-dependent diffusion coefficients D_A as indicated.

fusion coefficient of the defects involved in the particular reaction (see below). A contribution of a direct exchange is taken into account by D_A^{ex}. Equation (17) indicates that it can be difficult to identify the diffusion mechanisms of mainly substitutionally dissolved elements if several mechanisms contribute to diffusion simultaneously.

A more straightforward interpretation of D_A is obtained for the diffusion of A under an isoconcentration condition. In this case the diffusion is not affected by internal electric fields and/or chemical concentration gradients and always proceeds in thermal equilibrium, that is, the concentrations of native point defects are in thermal equilibrium. This diffusion peculiarity represents the foreign-atom controlled mode of diffusion (see below). Taking into account that the mobile defects are A_i^q, AV^j, and AI^v of reactions (1)–(7), the isoconcentration-diffusion coefficient D_A is given by

$$D_A = \frac{C_{A_i^q}^{\text{eq}} D_{A_i^q}}{C_{A_s^m}^{\text{eq}} + C_{A_i^q}^{\text{eq}}} + \frac{C_{AV^j}^{\text{eq}} D_{AV^j}}{C_{A_s^m}^{\text{eq}} + C_{AV^j}^{\text{eq}}} + \frac{C_{AI^v}^{\text{eq}} D_{AI^v}}{C_{A_s^m}^{\text{eq}} + C_{AI^v}^{\text{eq}}}. \tag{18}$$

This follows from the differential-equation system of the underlying reactions for the foreign-atom-controlled diffusion mode (see below). In the case that A is mainly dissolved on interstitial sites, i.e., $C_{A_i^q}^{\text{eq}} \gg C_{A_s^m}^{\text{eq}}, C_{AV^j}^{\text{eq}}, C_{AI^v}^{\text{eq}}$, and $D_{A_i^q} \gg D_{AV^j}, D_{AI^v}$, we get $D_A \approx D_{A_i^q}$ as expected for the diffusion via the direct interstitial mechanism. For a mainly substitutionally dissolved element ($C_{A_s^m}^{\text{eq}} \gg C_{A_i^q}^{\text{eq}}, C_{AV^j}^{\text{eq}}, C_{AI^v}^{\text{eq}}$) the diffusivity D_A is given by the sum of the reduced diffusion coefficients $D_X^* = C_X^{\text{eq}} D_X / C_{A_s^m}^{\text{eq}}$ with $X \in \{A_i^q, AV^j, AI^v\}$. Equation (18) describes, in particular, the isoconcentration diffusion of hybrid elements, which exist to a non-negligible extent both in mobile configurations and immobile substitutional sites. Then, however, usually one term on the right-hand side of Eq. (18) dominates. For example, the transport coefficient $C_{A_i^q}^{\text{eq}} D_{A_i^q}$ dominates for Au, Pt, and Zn diffusion in Si (Ref. 34) and for Cu, Ag, and Au diffusion in Ge.[32] In order to compare the diffusivities of different elements A in a semiconductor their diffusivities for isoconcentration conditions or for the foreign-atom-controlled diffusion mode are suitable measures.

C. Mathematical formulation of diffusion

The charge states of point defects become significant in dopant-diffusion processes when the solubility of the dopant A_s^m at diffusion temperature exceeds the intrinsic carrier concentration n_{in}. Then the Fermi level E_f deviates from its intrinsic position E_f^{in} and the material is denoted electronically extrinsic. Moving the Fermi level from its intrinsic position to a position under extrinsic conditions, the formation of charged-point defects X is affected and therewith their equilibrium concentrations C_X^{eq} and transport capacities $C_X^{\text{eq}} D_X$.[39] Moreover, the dopant profile creates an electric field, which additionally affects the diffusion of charged mobile defects. Accordingly, a drift of charged defects in the electric field must be added to Eq. (13), which then reads

$$J_X = -D_X \frac{\partial C_X}{\partial x} + \mu_X C_X \varepsilon(x). \tag{19}$$

Here μ and ε denote the mobility and the electric field, respectively. Taking into account that the electric field is the derivative of the potential ψ,

$$\varepsilon(x) = -\frac{\partial \psi(x)}{\partial x}, \tag{20}$$

and that the free-electron concentration is given by

$$n(x) = N_C \exp\left(\frac{E_f - E_C + e\psi(x)}{kT}\right), \tag{21}$$

with e being the elementary charge, the electric field can be written as

$$\varepsilon(x) = -\frac{kT}{e}\frac{1}{n(x)}\frac{\partial n(x)}{\partial x}. \tag{22}$$

Substituting Eq. (22) in Eq. (19) and using the Einstein relation,

$$\mu = ze\frac{D_X}{kT}, \tag{23}$$

with the charge state z of the diffusing species, we obtain

$$J_X = -D_X \frac{\partial C_X}{\partial x} - zC_X D_X \frac{1}{n(x)}\frac{\partial n(x)}{\partial x}. \tag{24}$$

In the case that the electric field is caused by acceptors, the flux equation reads

$$J_X = -D_X \frac{\partial C_X}{\partial x} + zC_X D_X \frac{1}{p(x)}\frac{\partial p(x)}{\partial x}, \tag{25}$$

where p denotes the free-hole concentration. Additional terms enter Eq. (19) when besides chemical and electrical forces also mechanical strain and/or hydrostatic pressure affect the flux of a point defect.

In the following the CT description of the diffusion of an element A is treated. Starting from the full differential-

equation system, useful approximations are applied to explain the relation between the shape of the diffusion profile and the charge states of the point defects involved in the particular diffusion process. An understanding of this relation is very helpful for getting first evidence on the mechanisms that can mediate the diffusion of element A.

D. The vacancy mechanism

The mathematical formulation of the vacancy mechanism (1) is described in this section representative of reactions (1)–(3). The treatment of reactions (2) and (3) equals that of reaction (1) since the interstitialcy and kick-out mechanisms have a reaction scheme, which is similar to the vacancy mechanism. Only the meaning of the model parameters changes. On the other hand, the dissociative mechanism (4) has a reaction scheme similar to the two dopant defect-pair-assisted mechanisms (6) and (7). The dissociative mechanism is treated exemplarily for the reactions (6) and (7) in Sec. II E.

The vacancy mechanism is given by reaction (1) in a generalized form. Adding the forward and backward rate constants, which are denoted k_+ and k_-, respectively, reaction (1) reads

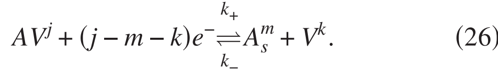

$$AV^j + (j-m-k)e^- \underset{k_-}{\overset{k_+}{\rightleftharpoons}} A_s^m + V^k. \tag{26}$$

Taking into account Eqs. (12) and (24), the following three coupled partial-differential equations describe the diffusion and reaction of the point defects involved in reaction (26):

$$\frac{\partial C_{A_s^m}}{\partial t} = \frac{\partial}{\partial x}\left(D_{A_s^m}\frac{\partial C_{A_s^m}}{\partial x} + m\frac{C_{A_s^m}D_{A_s^m}}{n(x)}\frac{\partial n(x)}{\partial x}\right) + k_+ C_{AV^j}C_o n^{(j-m-k)} - k_- C_{A_s^m}C_{V^k}n_{\text{in}}^{(j-m-k)}, \tag{27}$$

$$\frac{\partial C_{AV^j}}{\partial t} = \frac{\partial}{\partial x}\left(D_{AV^j}\frac{\partial C_{AV^j}}{\partial x} + j\frac{C_{AV^j}D_{AV^j}}{n(x)}\frac{\partial n(x)}{\partial x}\right) - k_+ C_{AV^j}C_o n^{(j-m-k)} + k_- C_{A_s^m}C_{V^k}n_{\text{in}}^{(j-m-k)}, \tag{28}$$

$$\frac{\partial C_{V^k}}{\partial t} = \frac{\partial}{\partial x}\left(D_{V^k}\frac{\partial C_{V^k}}{\partial x} + k\frac{C_{V^k}D_{V^k}}{n(x)}\frac{\partial n(x)}{\partial x}\right) + k_+ C_{AV^j}C_o n^{(j-m-k)} - k_- C_{A_s^m}C_{V^k}n_{\text{in}}^{(j-m-k)}, \tag{29}$$

where C_X (D_X) with $X \in \{A_s^m, AV^j, V^k\}$ is the concentration (diffusion coefficient) of the respective point defect.[40] C_o is the number density of substitutional lattice sites. The first term on the right-hand side of reactions (27)–(29) describes the change of the concentration of the point defect via diffusion and drift. The second term represents the formation (annihilation) of the point defect via reaction (26).

Introducing normalized concentrations $\widetilde{C}_X = C_X / C_X^{\text{eq}}$ and $\widetilde{n} = n/n^{\text{eq}}$, reduced diffusivities $D_X^* = C_X^{\text{eq}} D_X / C_{A_s^m}^{\text{eq}}$, and the relationship between the rate constants k_+ and k_-,

$$\frac{k_+}{k_-} = \frac{C_{A_s^m}^{\text{eq}} C_{V^k}^{\text{eq}} n_{\text{in}}^{(j-m-k)}}{C_{AV^j}^{\text{eq}} C_o (n^{\text{eq}})^{(j-m-k)}}, \tag{30}$$

due to the law of mass action, the differential equations (27)–(29) read

$$\frac{\partial \widetilde{C}_{A_s^m}}{\partial t} = \frac{\partial}{\partial x}\left(D_{A_s^m}\frac{\partial \widetilde{C}_{A_s^m}}{\partial x} + m\frac{\widetilde{C}_{A_s^m}D_{A_s^m}}{\widetilde{n}(x)}\frac{\partial \widetilde{n}(x)}{\partial x}\right) + k_- C_{V^k}^{\text{eq}} n_{\text{in}}^{(j-m-k)}(\widetilde{C}_{AV^j}\widetilde{n}^{(j-m-k)} - \widetilde{C}_{A_s^m}\widetilde{C}_{V^k}), \tag{31}$$

$$\frac{C_{AV^j}^{\text{eq}}}{C_{A_s^m}^{\text{eq}}}\frac{\partial \widetilde{C}_{AV^j}}{\partial t} = \frac{\partial}{\partial x}\left(D_{AV^j}^*\frac{\partial \widetilde{C}_{AV^j}}{\partial x} + j\frac{\widetilde{C}_{AV^j}D_{AV^j}^*}{\widetilde{n}(x)}\frac{\partial \widetilde{n}(x)}{\partial x}\right) - k_- C_{V^k}^{\text{eq}} n_{\text{in}}^{(j-m-k)}(\widetilde{C}_{AV^j}\widetilde{n}^{(j-m-k)} - \widetilde{C}_{A_s^m}\widetilde{C}_{V^k}), \tag{32}$$

$$\frac{C_{V^k}^{\text{eq}}}{C_{A_s^m}^{\text{eq}}}\frac{\partial \widetilde{C}_{V^k}}{\partial t} = \frac{\partial}{\partial x}\left(D_{V^k}^*\frac{\partial \widetilde{C}_{V^k}}{\partial x} + k\frac{\widetilde{C}_{V^k}D_{V^k}^*}{\widetilde{n}(x)}\frac{\partial \widetilde{n}(x)}{\partial x}\right) + k_- C_{V^k}^{\text{eq}} n_{\text{in}}^{(j-m-k)}(\widetilde{C}_{AV^j}\widetilde{n}^{(j-m-k)} - \widetilde{C}_{A_s^m}\widetilde{C}_{V^k}). \tag{33}$$

This differential-equation system describes the diffusion of A via the vacancy mechanism when A_s^m acts as a donor. For A_s^m being an acceptor, $\widetilde{n}$ and $\frac{1}{\widetilde{n}}\frac{\partial \widetilde{n}}{\partial x}$ are replaced by means of $np = n_{\text{in}}^2$ with $\frac{1}{\widetilde{p}}$ and $-\frac{1}{\widetilde{p}}\frac{\partial \widetilde{p}}{\partial x}$, respectively.

The electron and hole concentrations are related via the charge-neutrality equation

$$n = p + mC_{A_s^m} + kC_{V^k} + jC_{AV^j}, \tag{34}$$

with the concentrations of the point defects. For a substitutional donor A_s^m with $m \in \{+1, +2, \ldots\}$, we obtain

$$\widetilde{n}(x) = \frac{1}{2}\left(m\widetilde{C}_{A_s^m} + j\frac{C_{AV^j}^{\text{eq}}}{C_{A_s^m}^{\text{eq}}}\widetilde{C}_{AV^j} + k\frac{C_{V^k}^{\text{eq}}}{C_{A_s^m}^{\text{eq}}}\widetilde{C}_{V^k}\right) + \frac{1}{2}\sqrt{\left(m\widetilde{C}_{A_s^m} + j\frac{C_{AV^j}^{\text{eq}}}{C_{A_s^m}^{\text{eq}}}\widetilde{C}_{AV^j} + k\frac{C_{V^k}^{\text{eq}}}{C_{A_s^m}^{\text{eq}}}\widetilde{C}_{V^k}\right)^2 + 4\widetilde{n}_{\text{in}}^2},$$

$$\frac{1}{\widetilde{n}(x)}\frac{\partial \widetilde{n}(x)}{\partial x} = \frac{1}{\sqrt{\left(m\widetilde{C}_{A_s^m} + j\frac{C_{AV^j}^{\text{eq}}}{C_{A_s^m}^{\text{eq}}}\widetilde{C}_{AV^j} + k\frac{C_{V^k}^{\text{eq}}}{C_{A_s^m}^{\text{eq}}}\widetilde{C}_{V^k}\right)^2 + 4\widetilde{n}_{\text{in}}^2}} \times \frac{\partial\left(m\widetilde{C}_{A_s^m} + j\frac{C_{AV^j}^{\text{eq}}}{C_{A_s^m}^{\text{eq}}}\widetilde{C}_{AV^j} + k\frac{C_{V^k}^{\text{eq}}}{C_{A_s^m}^{\text{eq}}}\widetilde{C}_{V^k}\right)}{\partial x}, \tag{35}$$

and for a substitutional acceptor A_s^m with $m \in \{-1, -2, \ldots\}$,

$$\widetilde{p}(x) = \frac{1}{2}\left(-m\widetilde{C}_{A_s^m} - j\frac{C_{AV^j}^{eq}}{C_{A_s^m}^{eq}}\widetilde{C}_{AV^j} - k\frac{C_{V^k}^{eq}}{C_{A_s^m}^{eq}}\widetilde{C}_{V^k}\right) + \frac{1}{2}\sqrt{\left(-m\widetilde{C}_{A_s^m} - j\frac{C_{AV^j}^{eq}}{C_{A_s^m}^{eq}}\widetilde{C}_{AV^j} - k\frac{C_{V^k}^{eq}}{C_{A_s^m}^{eq}}\widetilde{C}_{V^k}\right)^2 + 4\widetilde{n}_{in}^2},$$

$$\frac{1}{\widetilde{p}(x)}\frac{\partial\widetilde{p}(x)}{\partial x} = \frac{1}{\sqrt{\left(-m\widetilde{C}_{A_s^m} - j\frac{C_{AV^j}^{eq}}{C_{A_s^m}^{eq}}\widetilde{C}_{AV^j} - k\frac{C_{V^k}^{eq}}{C_{A_s^m}^{eq}}\widetilde{C}_{V^k}\right)^2 + 4\widetilde{n}_{in}^2}} \times \frac{\partial\left(-m\widetilde{C}_{A_s^m} - j\frac{C_{AV^j}^{eq}}{C_{A_s^m}^{eq}}\widetilde{C}_{AV^j} - k\frac{C_{V^k}^{eq}}{C_{A_s^m}^{eq}}\widetilde{C}_{V^k}\right)}{\partial x}. \tag{36}$$

Equations (31)–(33) together with Eq. (35) [Eq. (36)] represent the full set of equations to calculate the diffusion profiles of donors (acceptors) A_s^m and of the other point defects in reaction (26) for specific initial and boundary conditions.

In order to highlight general aspects of dopant diffusion via the vacancy mechanism, approximations are considered in the following, which lead to a differential equation of the form of Eq. (14) with $G_X=0$. In particular, two different modes of dopant diffusion are distinguished. These are the native-defect controlled and foreign-atom controlled modes of diffusion. Each mode predicts characteristic diffusion profiles for A_s^m. The characteristic shape of the profiles reflects the charge states of the point defects controlling the diffusion process.

1. Native-defect-controlled diffusion mode

The vacancy-controlled mode of dopant diffusion is established when the relationship $D_{AV^j}^* \gg D_{V^k}^*$ holds. The higher transport capacity $C_{AV^j}^{eq} D_{AV^j}$ of the dopant-defect pair compared to $C_{V^k}^{eq} D_{V^k}$ leads to an almost homogeneous distribution of the dopant-vacancy pairs after sufficiently long diffusion times, i.e., $\widetilde{C}_{AV^j}\approx 1$. Accordingly, Eq. (32) can be neglected. The contribution of the direct diffusion of A_s^m to the total-diffusion coefficient D_A is generally small compared to the indirect diffusion via AV pairs. Taking the difference between Eqs. (31) and (33) and assuming $C_{V^k}^{eq} \ll C_{A_s^m}^{eq}$ we obtain

$$\frac{\partial\widetilde{C}_{A_s^m}}{\partial t} \approx -\frac{\partial}{\partial x}\left(D_{V^k}^*\frac{\partial\widetilde{C}_{V^k}}{\partial x} + k\frac{\widetilde{C}_{V^k}D_{V^k}^*}{\widetilde{n}(x)}\frac{\partial\widetilde{n}(x)}{\partial x}\right). \tag{37}$$

For local equilibrium of reaction (26),

$$\frac{\widetilde{C}_{A_s^m}\widetilde{C}_{V^k}}{\widetilde{C}_{AV^j}\widetilde{n}^{(j-m-k)}} = 1, \tag{38}$$

and of reaction $AV^j + je^- \rightleftharpoons AV^0$,

$$\frac{\widetilde{C}_{AV^0}}{\widetilde{C}_{AV^j}\widetilde{n}^j} = 1, \tag{39}$$

Eqs. (38) and (39) yield

$$\widetilde{C}_{V^k} = \frac{\widetilde{C}_{AV^0}\widetilde{n}^{(-m-k)}}{\widetilde{C}_{A_s^m}} \approx \frac{\widetilde{n}^{(-m-k)}}{\widetilde{C}_{A_s^m}}, \tag{40}$$

because $\widetilde{C}_{AV^0}\approx 1$. For high donor concentrations, i.e., $C_{A_s^m}^{eq}$ exceeds n_{in}, $\widetilde{n}\approx\widetilde{C}_{A_s^m}$ holds and Eq. (37) transforms with Eq. (40) to a differential equation of the form

$$\frac{\partial\widetilde{C}_{A_s^m}}{\partial t} - \frac{\partial}{\partial x}D_{A_s^m}^{eff}\frac{\partial\widetilde{C}_{A_s^m}}{\partial x} = 0, \tag{41}$$

with an effective diffusivity of A_s^m ($m\in\{+1,+2,\dots\}$) given by

$$D_{A_s^m}^{eff} = (m+1)D_{V^k}^*(\widetilde{C}_{A_s^m})^{-m-k-2}. \tag{42}$$

For high concentrations of an acceptor A_s^m ($m\in\{-1,-2,\dots\}$) with $\widetilde{p}\approx\widetilde{C}_{A_s^m}$, Eq. (41) with

$$D_{A_s^m}^{eff} = (-m+1)D_{V^k}^*(\widetilde{C}_{A_s^m})^{m+k-2} \tag{43}$$

is obtained.

2. Foreign-atom-controlled diffusion mode

The foreign-atom-controlled mode of dopant diffusion is established when the relationship $D_{AV^j}^* \ll D_{V^k}^*$ holds. The higher transport capacity of the vacancies compared to that of the dopant-defect pairs leads to an almost homogeneous distribution of V^k after sufficiently long times, i.e., $\widetilde{C}_{V^k}\approx 1$. Accordingly, Eq. (33) can be neglected. Taking into account that the direct diffusion of A_s^m is negligible compared to the indirect diffusion of A_s^m via AV pairs and that $C_{AV^j}^{eq} \ll C_{A_s^m}^{eq}$ holds, the sum of Eqs. (31) and (32) yields

$$\frac{\partial\widetilde{C}_{A_s^m}}{\partial t} \approx \frac{\partial}{\partial x}\left(D_{AV^j}^*\frac{\partial\widetilde{C}_{AV^j}}{\partial x} + j\frac{\widetilde{C}_{AV^j}D_{AV^j}^*}{\widetilde{n}(x)}\frac{\partial\widetilde{n}(x)}{\partial x}\right). \tag{44}$$

Assuming local equilibrium of reaction (26) and of the reaction $V^k + ke^- \rightleftharpoons V^0$, which is expressed by Eq. (38) and

$$\frac{\widetilde{C}_{V^0}}{\widetilde{C}_{V^k}\widetilde{n}^k} = 1, \tag{45}$$

respectively, one gets

$$\widetilde{C}_{AV^j} \approx \widetilde{C}_{A_s^m}\widetilde{n}^{(m-j)} = (\widetilde{C}_{A_s^m})^{(m-j+1)}. \tag{46}$$

For donors A_s^m($m=+1,+2,\dots$), with $\widetilde{n}\approx\widetilde{C}_{A_s^m}$, Eq. (44) transforms to Eq. (41) with

$$D^{\text{eff}}_{A^m_s} = (m+1) D^*_{AV^j} (\widetilde{C}_{A^m_s})^{m-j}. \tag{47}$$

For acceptors A^m_s ($m \in \{-1, -2, \ldots\}$) with $\widetilde{p} \approx \widetilde{C}_{A^m_s}$, the diffusion coefficient in Eq. (41) is given by

$$D^{\text{eff}}_{A^m_s} = (-m+1) D^*_{AV^j} (\widetilde{C}_{A^m_s})^{-m+j}. \tag{48}$$

E. Dissociative mechanism

The dissociative mechanism is representative for the mechanisms (4), (6), and (7), which all possess a similar reaction scheme. The partial-differential-equation system for modeling dopant diffusion via the dissociative mechanism is easily translated to the equation system for modeling diffusion via the dopant-defect pair assisted recombination mechanism (6) [mechanism (7)] by replacing the defect(s) A^q_i (A^q_i, V^k) with AI^v (AV^j, I^u).

Introducing forward and backward rate constants k_f and k_b, respectively, the dissociative mechanism reads

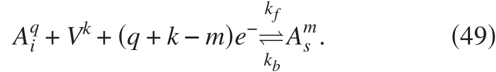

$$A^q_i + V^k + (q+k-m)e^- \underset{k_b}{\overset{k_f}{\rightleftharpoons}} A^m_s. \tag{49}$$

k_f and k_b are related via the law of mass action according to

$$\frac{k_f}{k_b} = \frac{C^{\text{eq}}_{A^m_s} C'_o n_{\text{in}}^{(q+k-m)}}{C^{\text{eq}}_{A^q_i} C^{\text{eq}}_{V^k} (n^{\text{eq}})^{(q+k-m)}}, \tag{50}$$

where C'_o is the number density of interstitial sites. Taking into account normalized concentrations and reduced diffusivities, the differential-equation system for modeling dopant diffusion via the dissociative mechanism (49) is

$$\frac{\partial \widetilde{C}_{A^m_s}}{\partial t} = \frac{\partial}{\partial x}\left(D_{A^m_s} \frac{\partial \widetilde{C}_{A^m_s}}{\partial x} + m \frac{\widetilde{C}_{A^m_s} D_{A^m_s}}{\widetilde{n}(x)} \frac{\partial \widetilde{n}(x)}{\partial x} \right) + k_b C'_o n_{\text{in}}^{(q+k-m)} \times (\widetilde{C}_{A^q_i} \widetilde{C}_{V^k} \widetilde{n}^{(q+k-m)} - \widetilde{C}_{A^m_s}), \tag{51}$$

$$\frac{C^{\text{eq}}_{A^q_i}}{C^{\text{eq}}_{A^m_s}} \frac{\partial \widetilde{C}_{A^q_i}}{\partial t} = \frac{\partial}{\partial x}\left(D^*_{A^q_i} \frac{\partial \widetilde{C}_{A^q_i}}{\partial x} + q \frac{\widetilde{C}_{A^q_i} D^*_{A^q_i}}{\widetilde{n}(x)} \frac{\partial \widetilde{n}(x)}{\partial x} \right) - k_b C'_o n_{\text{in}}^{(q+k-m)} \times (\widetilde{C}_{A^q_i} \widetilde{C}_{V^k} \widetilde{n}^{(q+k-m)} - \widetilde{C}_{A^m_s}), \tag{52}$$

$$\frac{C^{\text{eq}}_{V^k}}{C^{\text{eq}}_{A^m_s}} \frac{\partial \widetilde{C}_{V^k}}{\partial t} = \frac{\partial}{\partial x}\left(D^*_{V^k} \frac{\partial \widetilde{C}_{V^k}}{\partial x} + k \frac{\widetilde{C}_{V^k} D^*_{V^k}}{\widetilde{n}(x)} \frac{\partial \widetilde{n}(x)}{\partial x} \right) - k_b C'_o n_{\text{in}}^{(q+k-m)} \times (\widetilde{C}_{A^q_i} \widetilde{C}_{V^k} \widetilde{n}^{(q+k-m)} - \widetilde{C}_{A^m_s}). \tag{53}$$

The diffusion of a donor A^m_s ($m \in \{+1, +2, \ldots\}$) is described by Eqs. (51)–(53) and by equations for $\widetilde{n}$ and $\frac{1}{\widetilde{n}(x)} \frac{\partial \widetilde{n}(x)}{\partial x}$ that are similar to Eq. (35). For an acceptor A^m_s ($m \in \{-1, -2, \ldots\}$), $\widetilde{n}$ and $\frac{1}{\widetilde{n}} \frac{\partial \widetilde{n}}{\partial x}$ are replaced with $\frac{1}{\widetilde{p}}$ and $-\frac{1}{\widetilde{p}} \frac{\partial \widetilde{p}}{\partial x}$, respectively, and substituted by expressions similar to Eq. (36).

1. Native-defect-controlled diffusion mode

The native-defect-controlled mode of dopant diffusion exists when $D^*_{A^q_i} \gg D^*_{V^k}$ holds. The higher transport capacity $C^{\text{eq}}_{A^q_i} D_{A^q_i}$ compared to $C^{\text{eq}}_{V^k} D_{V^k}$ leads to $\widetilde{C}_{A^q_i} \approx 1$ after sufficiently long times. Under this condition we can neglect Eq. (52). Taking the sum of Eqs. (51) and (53) and assuming that the diffusion of A^m_s via direct exchange is small compared to the indirect diffusion of A^m_s via A^q_i and that $C^{\text{eq}}_{V^k} \ll C^{\text{eq}}_{A^m_s}$ is fulfilled, we obtain

$$\frac{\partial \widetilde{C}_{A^m_s}}{\partial t} \approx \frac{\partial}{\partial x}\left(D^*_{V^k} \frac{\partial \widetilde{C}_{V^k}}{\partial x} + k \frac{\widetilde{C}_{V^k} D^*_{V^k}}{\widetilde{n}(x)} \frac{\partial \widetilde{n}(x)}{\partial x} \right). \tag{54}$$

Considering local equilibrium of reaction (49) and $A^q_i + qe^- \rightleftharpoons A^0_i$,

$$\frac{\widetilde{C}_{A^m_s}}{\widetilde{C}_{A^q_i} \widetilde{C}_{V^k} \widetilde{n}^{(q+k-m)}} = 1, \tag{55}$$

$$\frac{\widetilde{C}_{A^0_i}}{\widetilde{C}_{A^q_i} \widetilde{n}^q} = 1, \tag{56}$$

we obtain

$$\widetilde{C}_{V^k} \approx \widetilde{C}_{A^m_s} \widetilde{n}^{(m-k)}. \tag{57}$$

For donors A^m_s ($m \in \{+1, +2, \ldots\}$) with $\widetilde{n}(x) \approx \widetilde{C}_{A^m_s}$, Eq. (54) transforms to Eq. (41) with

$$D^{\text{eff}}_{A^m_s} = (m+1) D^*_{V^k} (\widetilde{C}_{A^m_s})^{m-k}. \tag{58}$$

For acceptors A^m_s ($m \in \{-1, -2, \ldots\}$) with $\widetilde{p} \approx \widetilde{C}_{A^m_s}$, Eq. (41) with

$$D^{\text{eff}}_{A^m_s} = (-m+1) D^*_{V^k} (\widetilde{C}_{A^m_s})^{-m+k} \tag{59}$$

is obtained.

2. Foreign-atom-controlled diffusion mode

The foreign-atom-controlled mode of dopant diffusion via the dissociative mechanism is established when $D^*_{A^q_i} \ll D^*_{V^k}$ holds. Then, after sufficiently long times, thermal equilibrium of V^k is established, i.e., $\widetilde{C}_{V^k} \approx 1$ and we can neglect Eq. (53). Taking the sum of Eqs. (51) and (52) and assuming $C^{\text{eq}}_{A^q_i} \ll C^{\text{eq}}_{A^m_s}$ and $D_{A^m_s} (= D^{\text{ex}}_{A^m_s}) \approx 0$, we obtain

$$\frac{\partial \widetilde{C}_{A^m_s}}{\partial t} \approx \frac{\partial}{\partial x}\left(D^*_{A^q_i} \frac{\partial \widetilde{C}_{A^q_i}}{\partial x} + q \frac{\widetilde{C}_{A^q_i} D^*_{A^q_i}}{\widetilde{n}(x)} \frac{\partial \widetilde{n}(x)}{\partial x} \right). \tag{60}$$

With

$$\widetilde{C}_{A^q_i} \approx \widetilde{C}_{A^m_s} \widetilde{n}^{(m-q)}, \tag{61}$$

which results from Eqs. (45) and (55), Eq. (60) reduces to Eq. (41) with

TABLE I. Effective diffusion coefficients $D^{\mathrm{eff}}_{A_s^m}$ of the substitutional foreign atoms A_s^m obtained on the basis of the vacancy mechanism (1) for (a) the native-defect-controlled mode (see Sec. II D 1) and (b) the foreign-atom-controlled mode (see Sec. II D 2) of dopant diffusion. The concentration dependence of $D^{\mathrm{eff}}_{A_s^m}$ determines the shape of the dopant profile. Typical diffusion profiles of an element A are shown in Fig. 2.

Vacancy mechanism: $AV^j+(j-m-k)e^- \rightleftharpoons A_s^m+V^k$					
with $m=+1$(donor)			with $m=-1$(acceptor)		
Reaction	(a) $D^{\mathrm{eff}}_{A_s^m}$	(b) $D^{\mathrm{eff}}_{A_s^m}$	Reaction	(a) $D^{\mathrm{eff}}_{A_s^m}$	(b) $D^{\mathrm{eff}}_{A_s^m}$
$AV^0+e^- \rightleftharpoons A_s^+ + V^{2-}$	$2D^*_{V^{2-}}(\tilde{C}_{A_s^+})^{-1}$	$2D^*_{AV^0}(\tilde{C}_{A_s^+})^1$	$AV^0+e^- \rightleftharpoons A_s^- + V^0$	$2D^*_{V^0}(\tilde{C}_{A_s^-})^{-3}$	$2D^*_{AV^0}(\tilde{C}_{A_s^-})^1$
$AV^0 \rightleftharpoons A_s^+ + V^{1-}$	$2D^*_{V^-}(\tilde{C}_{A_s^+})^{-2}$	$2D^*_{AV^0}(\tilde{C}_{A_s^+})^1$	$AV^0 \rightleftharpoons A_s^- + V^+$	$2D^*_{V^+}(\tilde{C}_{A_s^-})^{-2}$	$2D^*_{AV^0}(\tilde{C}_{A_s^-})^1$
$AV^0-e^- \rightleftharpoons A_s^+ + V^0$	$2D^*_{V^0}(\tilde{C}_{A_s^+})^{-3}$	$2D^*_{AV^0}(\tilde{C}_{A_s^+})^1$	$AV^0-e^- \rightleftharpoons A_s^- + V^{2+}$	$2D^*_{V^{2+}}(\tilde{C}_{A_s^-})^{-1}$	$2D^*_{AV^0}(\tilde{C}_{A_s^-})^1$
$AV^- \rightleftharpoons A_s^+ + V^{2-}$	$2D^*_{V^{2-}}(\tilde{C}_{A_s^+})^{-1}$	$2D^*_{AV^-}(\tilde{C}_{A_s^+})^2$	$AV^+ + 2e^- \rightleftharpoons A_s^- + V^0$	$2D^*_{V^0}(\tilde{C}_{A_s^-})^{-3}$	$2D^*_{AV^+}(\tilde{C}_{A_s^-})^2$
$AV^- - e^- \rightleftharpoons A_s^+ + V^-$	$2D^*_{V^-}(\tilde{C}_{A_s^+})^{-2}$	$2D^*_{AV^-}(\tilde{C}_{A_s^+})^2$	$AV^+ + e^- \rightleftharpoons A_s^- + V^+$	$2D^*_{V^+}(\tilde{C}_{A_s^-})^{-2}$	$2D^*_{AV^+}(\tilde{C}_{A_s^-})^2$
$AV^- - 2e^- \rightleftharpoons A_s^+ + V^0$	$2D^*_{V^0}(\tilde{C}_{A_s^+})^{-3}$	$2D^*_{AV^-}(\tilde{C}_{A_s^+})^2$	$AV^+ \rightleftharpoons A_s^- + V^{2+}$	$2D^*_{V^{2+}}(\tilde{C}_{A_s^-})^{-1}$	$2D^*_{AV^+}(\tilde{C}_{A_s^-})^2$

$$D^{\mathrm{eff}}_{A_s^m} = (m+1) D^*_{A_i^q} (\tilde{C}_{A_s^m})^{m-q}. \quad (62)$$

This effective diffusivity holds for donors A_s^m ($m \in \{+1, +2, \ldots\}$) with $\tilde{n}(x) \approx \tilde{C}_{A_s^m}$.

For acceptors A_s^m ($m \in \{-1, -2, \ldots\}$) with $\tilde{p} \approx \tilde{C}_{A_s^m}$, $D^{\mathrm{eff}}_{A_s^m}$ in Eq. (41) is given by

$$D^{\mathrm{eff}}_{A_s^m} = (-m+1) D^*_{A_i^q} (\tilde{C}_{A_s^m})^{-m+q}. \quad (63)$$

F. General aspects of dopant diffusion in semiconductors

The effective diffusion coefficients $D^{\mathrm{eff}}_{A_s^m}$ for the vacancy (dissociative) mechanism in the native-defect-controlled mode given by Eqs. (42) and (43) [Eqs. (58) and (59)] reveal that dopant diffusion is affected by the charge states m and k of A_s^m and V^k. On the other hand, the foreign-atom controlled mode of dopant diffusion via the vacancy mechanism (dissociative mechanism) is determined by the charge states m and j (q) of A_s^m and AV^j (A_i^q), respectively [see Eqs. (47) and (48)] [Eqs. (62) and (63)]. Generally, the foreign-atom-controlled mode of dopant diffusion via reactions (1)–(4) and reactions (6) and (7) is not sensitive to the charge states of the native point defects. The equations derived in Secs. II D and II E for $D^{\mathrm{eff}}_{A_s^m}$ in the native-defect and foreign-atom-controlled diffusion mode confirm expressions for the effective dopant-diffusion coefficient given by Gösele.[26]

Tables I and II summarize the concentration dependence of $D^{\mathrm{eff}}_{A_s^m}$ for the vacancy mechanism and dissociative mechanism, respectively, taking into account charge states of point defects, which are relevant for dopant diffusion in semiconductors. The charge state m of A_s^m was chosen 1+ (1−) because singly ionized donors (acceptors) are commonly used for high n-type (p-type) doping of both elemental and compound semiconductors. It is emphasized that the concentra-

TABLE II. Effective diffusion coefficients $D^{\mathrm{eff}}_{A_s^m}$ of the substitutional foreign atoms A_s^m obtained on the basis of the dissociative mechanism (4) for (a) the native-defect-controlled mode (see Sec. II E 1) and (b) the foreign-atom-controlled mode (see Sec. II E 2) of dopant diffusion. The concentration dependence of $D^{\mathrm{eff}}_{A_s^m}$ determines the shape of the dopant-diffusion profile. Typical diffusion profiles of an element A are shown in Fig. 2.

Dissociative mechanism: $A_i^q+V^k+(q+k-m)e^- \rightleftharpoons A_s^m$					
with $m=+$(donor)			with $m=-1$(acceptor)		
Reaction	(a) $D^{\mathrm{eff}}_{A_s^m}$	(b) $D^{\mathrm{eff}}_{A_s^m}$	Reaction	(a) $D^{\mathrm{eff}}_{A_s^m}$	(b) $D^{\mathrm{eff}}_{A_s^m}$
$A_i^0+V^{2-}-3e^- \rightleftharpoons A_s^+$	$2D^*_{V^{2-}}(\tilde{C}_{A_s^+})^3$	$2D^*_{A_i^0}(\tilde{C}_{A_s^+})^1$	$A_i^0+V^0+e^- \rightleftharpoons A_s^-$	$2D^*_{V^0}(\tilde{C}_{A_s^-})^1$	$2D^*_{A_i^0}(\tilde{C}_{A_s^-})^1$
$A_i^0+V^- -2e^- \rightleftharpoons A_s^+$	$2D^*_{V^-}(\tilde{C}_{A_s^+})^2$	$2D^*_{A_i^0}(\tilde{C}_{A_s^+})^1$	$A_i^0+V^+ +2e^- \rightleftharpoons A_s^-$	$2D^*_{V^+}(\tilde{C}_{A_s^-})^2$	$2D^*_{A_i^0}(\tilde{C}_{A_s^-})^1$
$A_i^0+V^0-e^- \rightleftharpoons A_s^+$	$2D^*_{V^0}(\tilde{C}_{A_s^+})^1$	$2D^*_{A_i^0}(\tilde{C}_{A_s^+})^1$	$A_i^0+V^{2+}+3e^- \rightleftharpoons A_s^-$	$2D^*_{V^{2+}}(\tilde{C}_{A_s^-})^3$	$2D^*_{A_i^0}(\tilde{C}_{A_s^-})^1$
$A_i^-+V^{2-}-4e^- \rightleftharpoons A_s^+$	$2D^*_{V^{2-}}(\tilde{C}_{A_s^+})^3$	$2D^*_{A_i^-}(\tilde{C}_{A_s^+})^2$	$A_i^++V^0+2e^- \rightleftharpoons A_s^-$	$2D^*_{V^0}(\tilde{C}_{A_s^-})^1$	$2D^*_{A_i^+}(\tilde{C}_{A_s^-})^2$
$A_i^-+V^- -3e^- \rightleftharpoons A_s^+$	$2D^*_{V^-}(\tilde{C}_{A_s^+})^2$	$2D^*_{A_i^-}(\tilde{C}_{A_s^+})^2$	$A_i^++V^+ +3e^- \rightleftharpoons A_s^-$	$2D^*_{V^+}(\tilde{C}_{A_s^-})^2$	$2D^*_{A_i^+}(\tilde{C}_{A_s^-})^2$
$A_i^-+V^0-2e^- \rightleftharpoons A_s^+$	$2D^*_{V^0}(\tilde{C}_{A_s^+})^1$	$2D^*_{A_i^-}(\tilde{C}_{A_s^+})^2$	$A_i^++V^{2+}+4e^- \rightleftharpoons A_s^-$	$2D^*_{V^{2+}}(\tilde{C}_{A_s^-})^3$	$2D^*_{A_i^+}(\tilde{C}_{A_s^-})^2$

tion dependence of $D^{\text{eff}}_{A_s^m}$ deduced for the vacancy mechanism also holds for the interstitialcy (kick-out) mechanism given by reaction (2) [reaction (3)]. $D^{\text{eff}}_{A_s^m}$ for the interstitialcy (kick-out) mechanism is given by Table I when AV is changed to AI (A_i) and V is changed to I whereas the charge states of the defects are kept unchanged. On the other hand, $D^{\text{eff}}_{A_s^m}$ deduced for the dissociative mechanism and given in Table II also reflects $D^{\text{eff}}_{A_s^m}$ of the dopant-defect pair-assisted recombination mechanisms (6) and (7). This shows that Tables I and II are generally applicable to predict the concentration dependence of $D^{\text{eff}}_{A_s^m}$ for dopant diffusion via one of the mechanisms given by reactions (1)–(4) and reactions (6) and (7).

Table I reveals that $D^{\text{eff}}_{A_s^m}$ is proportional to $(C_{A_s^m})^r$ with $r \in \{-1,-2,-3\}$ for the native-defect-controlled mode of dopant diffusion via the vacancy mechanism. This power dependence is a consequence of the charge states of V^k under high n-type or p-type doping. A diffusion profile of an element A with a concentration-dependent diffusion coefficient D_A proportional to $(C_A)^{-2}$ is illustrated in Fig. 2. The dopant profile is characterized by a concave shape. On the other hand, the foreign-atom-controlled mode of dopant diffusion via the vacancy mechanism yields that $D^{\text{eff}}_{A_s^m}$ is proportional to $(C_{A_s^m})^r$ with $r \in \{1,2\}$. This power dependence results from the charge states of A_s^m and AV^j. The corresponding dopant profiles are characterized by a convex shape. This box shape gets more pronounced with increasing exponent r as demonstrated by the calculated profiles shown in Fig. 2.

In contrast to the vacancy mechanism, the dissociative mechanism predicts box-shaped diffusion profiles for singly ionized donors (acceptors) both for the native defect and foreign-atom-controlled diffusion mode in the case that neutral and negatively (positively) charged vacancies are favored under n-type (p-type) conditions (see Table II). More specifically, $D^{\text{eff}}_{A_s^m}$ is proportional to $(C_{A_s^m})^r$ with $r \in \{1,2,3\}$ when V^k with $k \in \{0,1-,2-\}$ ($k \in \{0,1+,2+\}$) mediate donor (acceptor) diffusion. In the foreign-atom-controlled mode $D^{\text{eff}}_{A_s^m}$ is also proportional to $(C_{A_s^m})^r$ with $r \in \{1+,2+\}$ when A_i^q is neutral and singly ionized, respectively. The power dependence results from the difference in the charge states between A_s^m and A_i^q, in the same way as for the vacancy mechanism. This demonstrates that the shape of dopant profile alone cannot tell which diffusion mode is operative.

The scheme of the concentration dependence of $D^{\text{eff}}_{A_s^m}$ given by Tables I and II is very helpful for the understanding of dopant profiles in Si and Ge and its alloys. The scheme also holds for dopant diffusion in compound semiconductors such as SiC,GaAs,GaSb,... in the case the diffusion process is restricted to one sublattice. Also charge states of point defects other than those considered in Tables I and II may become important. Then the corresponding concentration dependence of $D^{\text{eff}}_{A_s^m}$ is given by Eqs. (42), (43), (58), and (59) for the native-defect-controlled mode and by Eqs. (47), (48), (62), and (63) for the foreign-atom-controlled mode.

It is evident from Tables I and II that the shape of the profile alone is not sufficient to identify the mechanisms of diffusion. A detailed analysis should include a direct comparison of the experimental profiles with numerical solutions of the full partial-differential-equation system and a comparison of the reduced diffusion coefficients D_X^* with self-diffusion data. In general, several mechanisms can contribute to dopant diffusion, which complicates the characterization of the underlying mechanisms. In order to obtain comprehensive information about the nature of the point defects, additional diffusion studies under various experimental conditions must be performed. In this respect investigations of the impact of self-interstitial and vacancy perturbations on dopant diffusion are advantageous. Such experiments were extensively performed with silicon.[1] Oxidation (nitridation) of a bare Si surface is known to inject self-interstitials (vacancies). The results considerably contributed to our present understanding of dopant diffusion in this elemental semiconductor (see e.g., Refs. 41–49).

Recently, a new approach of studying dopant diffusion in semiconductors was proposed by the author. These experiments concern diffusion studies with isotopically enriched semiconductor multilayer structures.[50–55] By means of these structures the impact of dopant diffusion on self-diffusion can be investigated directly. Modeling of the simultaneous self- and dopant diffusion is more complex than modeling of the separate processes but is a worthwhile effort because more information about the underlying mechanisms and properties of the point defects is obtained than from self- and dopant-diffusion experiments studied separately.[54,55] The mathematical treatment of the simultaneous diffusion is described in the following section. Theoretical profiles are presented for a dopant that diffuses via the interstitialcy and vacancy mechanisms. The calculations help to understand the relation between self- and dopant diffusion and demonstrate the potency of this new approach of studying dopant diffusion. Specific experimental results obtained from modeling dopant diffusion in Si isotope multilayer structures are presented in Part II.

III. SIMULTANEOUS SELF- AND DOPANT DIFFUSION

A. Impact of doping on the formation of point defects

In the case when a foreign atom diffuses into a semiconductor with an isotopically enriched multilayer structure, the diffusion of host atoms can be affected both by point-defect reactions and doping. The incorporation of foreign atoms on substitutional sites takes place via the formation (annihilation) of native-point defects. This can lead to native-defect concentrations, which deviate from thermal equilibrium. As a consequence the self-diffusion is enhanced (retarded) compared to self-diffusion under thermal equilibrium. Additionally, a high concentration of electrically active foreign atoms can give rise to free-charge carriers that exceed the intrinsic carrier concentration. As a consequence the position of the Fermi level deviates from its intrinsic position E_f^{in} and, therewith, the ratio of charged- to neutral-defect concentrations in thermal equilibrium changes. For donors X^{z+} and acceptors X^{z-} with charge states $z \in \{1,2,\ldots\}$ and energy levels $E_{X^{z+}}$ and $E_{X^{z-}}$ above the valence band E_v, this ratio reads[39]

$$\frac{C^{\mathrm{eq}}_{X^{z+}}}{C^{\mathrm{eq}}_{X^0}} = g_{X^{z+}} \exp\left(-\frac{zE_f - \sum_{i=1}^{z} E_{X^{i+}}}{kT}\right) = g_{X^{z+}} \exp\left(-\frac{zE_f^{\mathrm{in}} - \sum_{i=1}^{z} E_{X^{i+}}}{kT}\right)\left(\frac{n_{\mathrm{in}}}{n^{\mathrm{eq}}}\right)^{z}, \quad (64)$$

and

$$\frac{C^{\mathrm{eq}}_{X^{z-}}}{C^{\mathrm{eq}}_{X^0}} = \frac{1}{g_{X^{z-}}} \exp\left(\frac{zE_f - \sum_{i=1}^{z} E_{X^{i-}}}{kT}\right) = \frac{1}{g_{X^{z-}}} \exp\left(\frac{zE_f^{\mathrm{in}} - \sum_{i=1}^{z} E_{X^{i-}}}{kT}\right)\left(\frac{n_{\mathrm{in}}}{p^{\mathrm{eq}}}\right)^{z}, \quad (65)$$

respectively, where n^{eq} (p^{eq}) represent the maximum free-electron (hole) concentration. For high n-type (p-type) doping levels n^{eq} (p^{eq}) approximates the donor (acceptor) concentration $C^{\mathrm{eq}}_{A_s^m}$ [see Eq. (77)]. The thermal-equilibrium concentrations of the neutral defects $C^{\mathrm{eq}}_{X^0}$ are independent of the position of the Fermi level E_f and given by

$$C^{\mathrm{eq}}_{X^0} = \exp\left(-\frac{G^F_{X^0}}{kT}\right), \quad (66)$$

where $G^F_{X^0}$ is the free enthalpy of the formation of X^0. The degeneracy factor g_X takes into account both the spin degeneracy of the defect and the degeneracy of the conduction and the valence band. Equations (64) and (65) indicate that the concentrations of donors and acceptors decrease (increase) under n- and p-type doping (p- and n-type doping), respectively. Substituting Eq. (66) in Eqs. (64) and (65) it becomes evident that the Fermi level alters the formation energy of a charged defect. This impact of E_f on the formation of charged-point defects is called the Fermi-level effect.

The total thermal-equilibrium concentration C^{eq}_X of X is given by the sum of the various contributions due to the different charge states,

$$C^{\mathrm{eq}}_X = C^{\mathrm{eq}}_{X^0}\left(1 + \sum_{i=1}^{z} \frac{C^{\mathrm{eq}}_{X^{i+}}}{C^{\mathrm{eq}}_{X^0}} + \sum_{i=1}^{z} \frac{C^{\mathrm{eq}}_{X^{i-}}}{C^{\mathrm{eq}}_{X^0}}\right). \quad (67)$$

Taking into account Eqs. (64) and (65), C^{eq}_X can be calculated for a specific doping level when $C^{\mathrm{eq}}_{X^0}$, the energy levels E_X, and degeneracy factors g_X are known. The total transport capacity $C^{\mathrm{eq}}_X D_X$ is given by a similar relationship,

$$C^{\mathrm{eq}}_X D_X = C^{\mathrm{eq}}_{X^0} D_{X^0}\left(1 + \sum_{i=1}^{z} \frac{C^{\mathrm{eq}}_{X^{i+}} D_{X^{i+}}}{C^{\mathrm{eq}}_{X^0} D_{X^0}} + \sum_{i=1}^{z} \frac{C^{\mathrm{eq}}_{X^{i-}} D_{X^{i-}}}{C^{\mathrm{eq}}_{X^0} D_{X^0}}\right). \quad (68)$$

Assuming that the diffusion coefficients of X are approximately equal for the various charge states, i.e., $D_{X^0} \approx D_{X^{i\pm}}$, it follows

$$C^{\mathrm{eq}}_X D_X \approx C^{\mathrm{eq}}_{X^0} D_{X^0}\left(1 + \sum_{i=1}^{z} \frac{C^{\mathrm{eq}}_{X^{i+}}}{C^{\mathrm{eq}}_{X^0}} + \sum_{i=1}^{z} \frac{C^{\mathrm{eq}}_{X^{i-}}}{C^{\mathrm{eq}}_{X^0}}\right). \quad (69)$$

With Eqs. (64), (65), and (69), $C^{\mathrm{eq}}_X D_X$ can be calculated for a specific doping level when $C^{\mathrm{eq}}_{X^0} D_{X^0}$ and the energy levels E_X are known. On the other hand, the energy levels can be calculated when the degeneracy factors of X, the total transport capacity $C^{\mathrm{eq}}_X D_X$ and its individual contributions are known provided that $D_{X^0} \approx D_{X^{i\pm}}$ holds.

Considering the ratio $C^{\mathrm{eq}}_{X^z}/C^{\mathrm{eq,in}}_{X^z}$ between the equilibrium concentration of X for extrinsic and intrinsic doping conditions, Eqs. (64) and (65) yield

$$\frac{C^{\mathrm{eq}}_{X^z}}{C^{\mathrm{eq,in}}_{X^z}} = \left(\frac{n_{\mathrm{in}}}{n^{\mathrm{eq}}}\right)^{z}, \quad (70)$$

with $z \in \{\pm 1, \pm 2, \ldots\}$. The ratio of the equilibrium concentration of X^z for extrinsic and intrinsic doping does not depend on the defect-energy levels. The transport capacity $C^{\mathrm{eq}}_{X^z} D_{X^z}$ and reduced-diffusion coefficient $D^*_{X^z} = C^{\mathrm{eq}}_{X^z} D_{X^z} / C^{\mathrm{eq}}_{A_s^m}$ for extrinsic doping are associated with their intrinsic quantities $C^{\mathrm{eq,in}}_{X^z} D_{X^z}$ and $D^*_{X^z}(n_{\mathrm{in}})$ via

$$C^{\mathrm{eq}}_{X^z} D_{X^z} = C^{\mathrm{eq,in}}_{X^z} D_{X^z}\left(\frac{n^{\mathrm{eq}}}{n_{\mathrm{in}}}\right)^{-z}, \quad (71)$$

$$D^*_{X^z} = \frac{C^{\mathrm{eq}}_{X^z} D_{X^z}}{C^{\mathrm{eq}}_{A_s^m}} = \frac{C^{\mathrm{eq,in}}_{X^z} D_{X^z}}{C^{\mathrm{eq,in}}_{A_s^m}}\left(\frac{n^{\mathrm{eq}}}{n_{\mathrm{in}}}\right)^{m-z} = D^*_{X^z}(n_{\mathrm{in}})\left(\frac{n^{\mathrm{eq}}}{n_{\mathrm{in}}}\right)^{m-z}. \quad (72)$$

With Eqs. (71) and (72) $C^{\mathrm{eq}}_{X^z} D_{X^z}$ and $D^*_{X^z}$ can be calculated for any doping level when their intrinsic values are known. For p-type doping, n^{eq} in Eqs. (70)–(72) is expressed by means of $n^{\mathrm{eq}} p^{\mathrm{eq}} = (n_{\mathrm{in}})^2$ with p^{eq}.

B. Impact of doping on self-diffusion

For modeling the simultaneous diffusion of self- and dopant atoms in semiconductor isotope structures, the self-diffusion equation together with the equations for dopant diffusion must be solved. According to Eq. (14) the diffusion of self-atoms is described by

$$\frac{\partial C_Z}{\partial t} - \frac{\partial}{\partial x} D_Z \frac{\partial C_Z}{\partial x} = 0, \quad (73)$$

where Z denotes the self-atom in an elemental semiconductor such as Si and Ge or the self-atom on the sublattice of a

compound semiconductor. Since the concentration of dopants is generally small compared to the number of host atoms, the self-atom concentration is not significantly affected by the formation of A_s^m. Accordingly, the change of the host-atom concentration via reactions (1)–(4) and reactions (6) and (7) is neglected in Eq. (73). However, dopant-defect pairs such as AV^j and AI^v may contribute to self-diffusion. Taking into account the contributions of V^k, I^u, AV^j, and AI^v, the self-diffusion coefficient is

$$D_Z=\left(\sum_k f_{V^k}C_{V^k}D_{V^k}+\sum_u f_{I^u}C_{I^u}D_{I^u}\right)\frac{1}{C_o} + \left(\sum_j f_{AV^j}C_{AV^j}D_{AV^j}+\sum_v f_{AI^v}C_{AI^v}D_{AI^v}\right)\frac{1}{C_o}, \quad (74)$$

where f_V, f_I, f_{AV}, and f_{AI} are the diffusion-correlation factors of the particular defect. The sum reflects the contributions of the different charged defects. With $\tilde{C}_X=C_X/C_X^{\text{eq}}$ and $D_X^*=C_X^{\text{eq}}D_X/C_{A_s^m}^{\text{eq}}$ $(X\in\{AV^j,AI^v,V^k,I^u\})$ the self-diffusion coefficient reads

$$D_Z=\left(\sum_k f_{V^k}D_{V^k}^*\tilde{C}_{V^k}+\sum_u f_{I^u}D_{I^u}^*\tilde{C}_{I^u}\right)\frac{C_{A_s^m}^{\text{eq}}}{C_o} + \left(\sum_j f_{AV^j}D_{AV^j}^*\tilde{C}_{AV^j}+\sum_v f_{AI^v}D_{AI^v}^*\tilde{C}_{AI^v}\right)\frac{C_{A_s^m}^{\text{eq}}}{C_o}. \quad (75)$$

This expression of D_Z is advantageous for numerically solving the differential equations of the simultaneous self- and dopant-atom diffusion because it contains the same model parameters D_X^* and variables $\tilde{C}_X$, which also enter the equation system of the vacancy mechanism [see Eqs. (31)–(33)] and the dissociative mechanism [see Eqs. (51)–(53)].

C. Simulation

For the simulation of self- and dopant diffusion in a semiconductor isotope heterostructure the formation of a substitutionally dissolved single acceptor $A_s^-(m=-1)$ via reactions (2) and (6) is considered. The dopant-defect pair is assumed to exist in neutral and singly positively charged states, i.e., $AI^v\in\{AI^0,AI^+\}$. Various charge states are taken into account for the self-interstitials $I^u\in\{I^-,I^0,I^+,I^{2+}\}$ and vacancies $V^k\in\{V^-,V^0,V^+,V^{2+}\}$. This amounts to 11 different point defects involved in the diffusion process. Accordingly, we get a system of 11 differential equations. Compared to Eqs. (31)–(33) and Eqs. (51)–(53), the differential equations contain additional terms, which account for the formation (annihilation) of the point defects via the various reactions. The numerical solution of the equation system is determined by the boundary and initial concentrations of the point defects and the settings of the model parameters. In order to model the diffusion of an acceptor into an undoped semiconductor it is assumed that the equilibrium concentrations for extrinsic doping conditions are instantaneously established at the surface, i.e., $\tilde{C}_X(x=0,t)=1$ with $X\in\{A_s^-,AI^v,V^k,I^u\}$. The initial concentrations of V^k and I^u are set to the thermal equilibrium

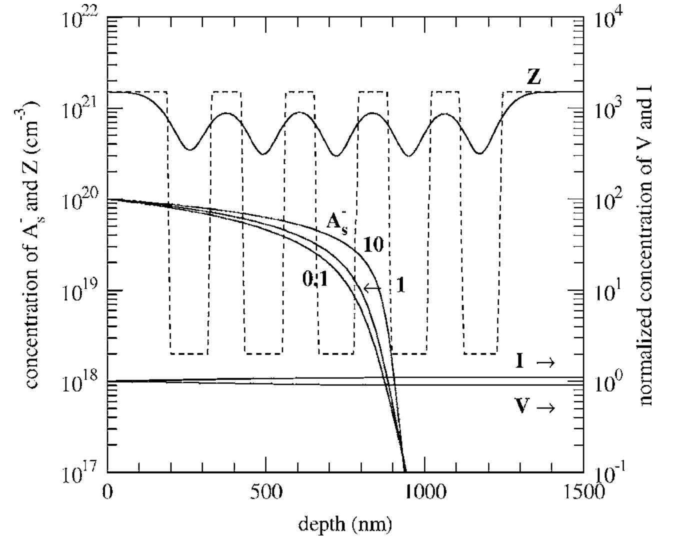

FIG. 3. Numerical calculations of the simultaneous diffusion of foreign atoms A and self-atoms Z in an isotope multilayer structure for the foreign-atom-controlled diffusion mode. The dashed line represents the initial distribution of the self-atoms. The diffusion of A proceeds via mobile AI^v pairs with charge states $v\in\{0,+1\}$. Single acceptors A_s^- are formed via reactions (2) and (6), which only involve neutral native-point defects. A_s^- profiles (solid lines) obtained for $D_{AI^+}^*/D_{AI^0}^*=0.1$, 1, and 10 confirm the concentration dependence of $D_{A_s^-}^{\text{eff}}$ derived in Secs. II D 2 and II E 2. The corresponding self-atom profile (upper solid line) indicates a homogeneous broadening, which shows that the concentrations of neutral native defects (lower solid lines) are close to thermal equilibrium.

under intrinsic conditions, i.e., $\tilde{C}_{V^k}(x>0,t=0)=C_{V^k}^{\text{eq,in}}/C_{V^k}^{\text{eq}}=(n_{\text{in}}/p^{\text{eq}})^k$ and $\tilde{C}_{I^u}(x>0,t=0)=C_{I^u}^{\text{eq,in}}/C_{I^u}^{\text{eq}}=(n_{\text{in}}/p^{\text{eq}})^u$.[56] The initial concentration of A_s^- is set to $\tilde{C}_{A_s^-}(x>0,t=0)=10^{-10}$ and therewith below the detection limit of common instruments for trace analysis. Prior to the diffusion process, reactions (2) and (6) are in local equilibrium. Accordingly, the initial concentration of AI^v is given by

$$\tilde{C}_{AI^v}(x>0,t=0)=[\tilde{p}(x>0,t=0)]^{(v-u+1)}10^{-10}. \quad (76)$$

$\tilde{p}(x>0,t=0)=n_{\text{in}}/p^{\text{eq}}$ denotes the normalized initial free-hole concentration with the maximum free-hole concentration

$$p^{\text{eq}}=\frac{1}{2}(C_{A_s^-}^{\text{eq}}-kC_{V^k}^{\text{eq}}-uC_{I^u}^{\text{eq}}-vC_{AI^v}^{\text{eq}}) + \frac{1}{2}\sqrt{(C_{A_s^-}^{\text{eq}}-kC_{V^k}^{\text{eq}}-uC_{I^u}^{\text{eq}}-vC_{AI^v}^{\text{eq}})^2+4n_{\text{in}}^2}. \quad (77)$$

Assuming that $C_X^{\text{eq}}(X\in\{V^k,I^u,AI^v\})$ is small compared to $C_{A_s^-}^{\text{eq}}$ and that $C_{A_s^-}^{\text{eq}}$ significantly exceeds n_{in}, then $p^{\text{eq}}\approx C_{A_s^-}^{\text{eq}}$ holds. This is in many cases a good approximation for extrinsic doping conditions.

The differential-equation system is solved numerically using a software package provided by Jüngling *et al.*[57] Additionally, Eq. (73) with D_Z given by Eq. (75) is solved. For the

initial concentration of the host atoms the distribution illustrated by the dashed line in Fig. 3 is used. This describes a ^{30}Si profile in a ^{nat}Si/^{28}Si multilayer structure.[54] The structure was used for the investigation of the simultaneous diffusion of self- and dopant atoms in Si.[50–55] Diffusion times of several minutes were assumed that are sufficient to establish local equilibrium of reactions (2) and (6). Under these conditions the reaction rates do not affect the shape of the calculated profiles. The diffusion of A_s^- via direct exchange with adjacent lattice atoms was neglected compared to the indirect diffusion of A_s^-, i.e., $D_{A_s^-} \approx 0$. The remaining model parameters of the differential equations are the reduced diffusion coefficients $D_X^* = C_X^{eq} D_X / C_{A_s^-}^{eq}$ and reduced equilibrium concentrations $C_X^{eq}/C_{A_s^-}^{eq}$ with $X \in \{AI^v, V^k, I^u\}$. The parameter $C_{AI^v}^{eq}/C_{A_s^-}^{eq}$ is set to 10^{-3}. This is certainly a good approximation for a mainly substitutionally dissolved dopant. Values several orders of magnitude lower were used for $C_{I^u}^{eq}/C_{A_s^-}^{eq}$ and $C_{V^k}^{eq}/C_{A_s^-}^{eq}$. With these settings for $C_X^{eq}/C_{A_s^-}^{eq}$, the calculated profiles $\tilde{C}_{A_s^-}$ are fairly insensitive to the equilibrium concentrations C_X^{eq} (Ref. 58) and the dopant profile is mainly determined by $D_X^* = C_X^{eq} D_X / C_{A_s^-}^{eq}$ ($X \in \{AI^v, V^k, I^u\}$). In the case that the equilibrium concentrations of native-point defects is several orders of magnitude higher, dopant diffusion can be sensitive to the native defect concentration. An example is the diffusion of Zn in GaSb.[59] Details about this study will be published elsewhere. In the following, simulations of dopant diffusion via reactions (2) and (6) under the above-mentioned constraints are shown for the foreign-atom and native-defect-controlled modes and, in addition, for an intermediate diffusion mode.

1. Foreign-atom-controlled mode

For the simulation of the foreign-atom-controlled dopant diffusion via reactions (2) and (6) the model parameters D_X^* were set according to the relationship $D_{AI^v}^* \ll D_{V^k,I^u}^*$, which must hold for this mode. Figure 3 illustrates calculated concentration profiles of A_s^-. The numerical solution of the differential-equation system also provides the corresponding concentration profiles of V^k and I^u. Figure 3 reveals that their concentrations are close to thermal equilibrium, i.e., $\tilde{C}_{V^k,I^u} \approx 1$, indicating that the foreign-atom-controlled diffusion mode is established. Simulations were performed with different values of $D_{AI^+}^*/D_{AI^0}^*$. The shape of the dopant profile becomes more box-shaped when the contribution of AI^+ pairs to dopant diffusion exceeds that of AI^0. The dopant profile calculated for $D_{AI^+}^*/D_{AI^0}^* = 0.1$ reflects an effective diffusivity $D_{A_s^-}^{eff}$ that is proportional to $C_{A_s^-}$. For $D_{AI^+}^*/D_{AI^0}^* = 10$ the apparent diffusion coefficient of A_s^- is proportional to $(C_{A_s^-})^2$. This dependence of the dopant profile on the difference in charge of A_s^- and AI^v confirms the expressions derived for $D_{A_s^m}^{eff}$ in Secs. II D 2 and II E 2. In addition to the A_s^- profile, the diffusion of self-atoms via vacancies and self-interstitials was calculated. The initial self-atom distribution (see the dashed line in Fig. 3) is representative for an isotope multilayer structure. In the case when both vacancies and self-interstitials are neutral even under extrinsic doping, a homogeneous broadening of the multilayer structure is expected that is confirmed by the calculations.

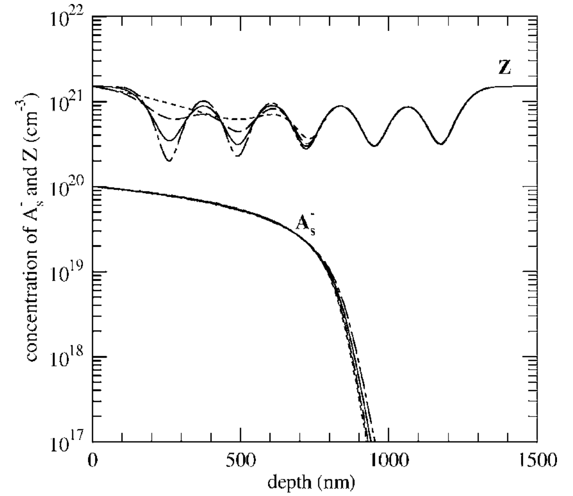

FIG. 4. Numerical calculations of the simultaneous diffusion of foreign atoms A and self-atoms Z in an isotope multilayer structure for the foreign-atom-controlled mode. The simulations were performed for $D_{AI^+}^*/D_{AI^0}^* = 1$. Only V^0 and I^0 (solid lines), I^+ (wide-dashed lines), I^{2+} (short-dashed lines), or I^- (long-short-dashed lines) were taken into account in reactions (2) and (6). Whereas the A_s^- profile is fairly insensitive to the charge states of the native-point defects, the self-diffusion within the extrinsic region of the acceptor profile depends on the charge state of I. The observed slight deviation among the A_s^- profiles is due to small variations in the corresponding profiles of V and I (not shown).

Figure 4 shows simulations for $D_{AI^+}^*/D_{AI^0}^* = 1.0$ assuming that only neutral native-point defects (solid lines) or both neutral and charged self-interstitial (dashed lines) are involved in reactions (2) and (6). The simulations reveal that the A_s^- profiles and the corresponding V and I profiles (not shown) are fairly insensitive to the charge states of V and I. However, the diffusion of the self-atoms within the extrinsic region of the dopant profile is clearly sensitive to the charge states of I^u. For singly positively charged self-interstitials that introduce a donor level in the middle of the band gap, the concentration of I^+ increases with increasing p-type doping. As a consequence the self-diffusion is enhanced (upper wide dashed line) compared to intrinsic conditions (upper solid line). Self-diffusion is even more enhanced within the dopant-diffused region when doubly positively charged self-interstitials I^{2+} dominate (see upper short-dashed line in Fig. 4). If I^- exists, the self-diffusion is retarded within the extrinsic region of the dopant profile (upper long-short dashed line).

The simulations illustrated in Figs. 3 and 4 demonstrate that the diffusion of an element A, which proceeds in a foreign-atom-controlled mode ($D_{AI^v}^* \ll D_{V^k,I^u}^*$), can*not* provide any information about native-point defects. However, the charge states of the native-point defects become apparent when the dopant diffuses into an isotope structure. This is experimentally confirmed by the diffusion of As in Si isotope

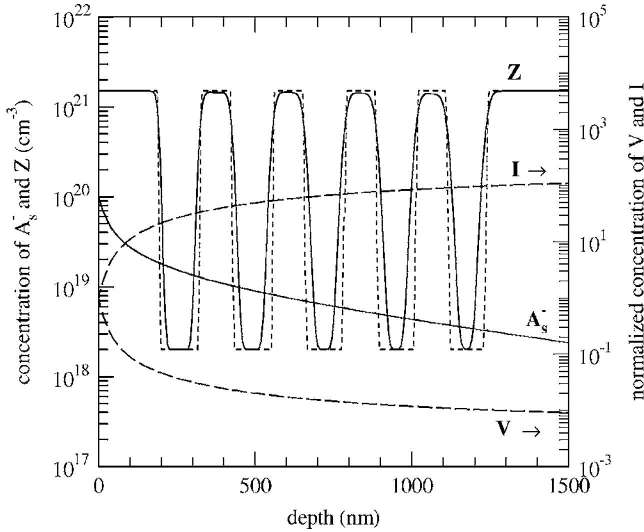

FIG. 5. Numerical calculations of the simultaneous diffusion of foreign atoms A and self-atoms Z in an isotope multilayer structure for the native-defect-controlled mode. The simulations were performed on the basis of reactions (2) and (6) with AI^0, A_s^-, V^0, and I^0. The short-dashed line indicates the initial distribution of the self-atoms. The enhanced self-diffusion with increasing penetration depth (upper solid line) is due to the I supersaturation (upper long-dashed line). The concave shape of the A_s^- profile (lower solid line) is mainly determined by reaction (2). This reaction leads to a concentration dependence of $D_{A_s^-}^{\mathrm{eff}} \propto (\widetilde{C}_{A_s^-})^{-3}$ (see the right-hand side of Table I).

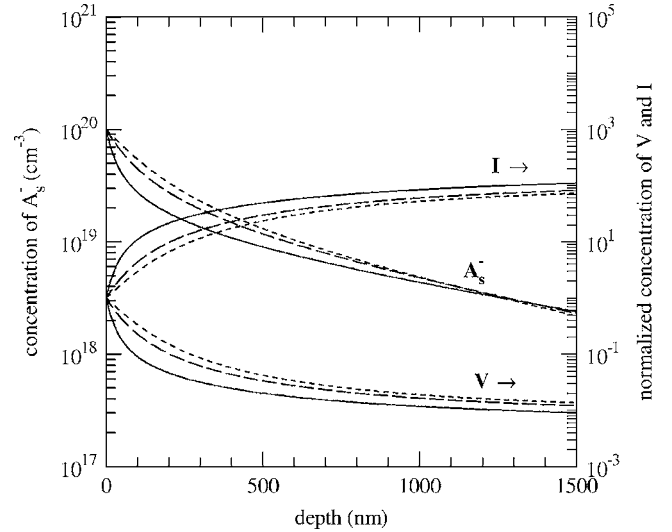

FIG. 6. Numerical calculations of the diffusion of A_s^-, V, and I performed on the basis of reactions (2) and (6) for the native-defect-controlled diffusion mode. The solid lines show the results for V^0 and I^0. The long-dashed and short-dashed lines represent calculations for I^+ and I^{2+}, respectively. The shape of the A_s^- profiles changes from $D_{A_s^-}^{\mathrm{eff}} \propto (\widetilde{C}_{A_s^-})^{-3}$, $\propto (\widetilde{C}_{A_s^-})^{-2}$, and $\propto (\widetilde{C}_{A_s^-})^{-1}$ with increasing charge state.

multilayer structures (see Part II). Nevertheless, it is difficult to specify the nature and properties of native-point defects from the foreign-atom-controlled diffusion of dopants into an isotope structure when both vacancies and self-interstitials contribute to self-diffusion. Then diffusion conditions yielding a dominance of one type of native defect are advantageous. Provided that the native defect controls dopant diffusion the simultaneous diffusion of self- and dopant atoms yields unambiguous information about the properties of the native defect. This native-defect-controlled mode of dopant diffusion can be realized by an athermal generation of defects via particle irradiation or via specific surface reactions. In addition, this mode can be established by the diffusion mechanism itself since all reactions (1)–(7) act as sinks (sources) for native defects. In the following, simulations for the native-defect-controlled mode of dopant diffusion and its impact on self-diffusion are shown. Experiments in this line help to identify the type and charge states of native-point defects involved in the diffusion process (see Part II).

2. Native-defect-controlled mode

For the simulation of the native-defect-controlled mode of dopant diffusion via reactions (2) and (6) the model parameters D_X^* were set according to the relationship $D_{AI^v}^* \gg D_{V^k,I^u}^*$. First we consider that the charge states of V and I are neutral. Then extrinsic doping will not affect self-diffusion. However, the concentration of V and I associated with the formation of A_s^- can significantly deviate from thermal equilibrium. Figure 5 shows corresponding simulations of dopant diffusion in an isotope structure. An enhanced self-diffusion with increasing penetration depth is observed. This enhancement is due to the I supersaturation, which is created by the formation of A_s^- via reaction (2). The inhomogeneous broadening of the multilayer structure reflects the deviation of the native-defect concentration from thermal equilibrium. This deviation is visualized by the normalized concentrations of V and I shown in Fig. 5 (see the long-dashed lines). The supersaturation (undersaturation) of I (V) raises (suppresses) the contribution of reaction (2) [reaction (6)] to the formation of A_s^-. Accordingly, the A_s^- profile is mainly determined by reaction (2). The concave shape of the A_s^- profile is in accord with a concentration dependence of $D_{A_s^-}^{\mathrm{eff}} \propto (\widetilde{C}_{A_s^-})^{-3}$. This confirms the predictions for $D_{A_s^-}^{\mathrm{eff}}$ derived for the interstitialcy mechanism[60] when a neutral self-interstitial is assumed (see the right-hand side of Table I). For I^+ and I^{2+} the simulations yield A_s^- profiles whose shape changes according to $D_{A_s^-}^{\mathrm{eff}} \propto (\widetilde{C}_{A_s^-})^{-2}$ and $D_{A_s^-}^{\mathrm{eff}} \propto (\widetilde{C}_{A_s^-})^{-1}$, respectively. This is demonstrated by the profiles shown in Fig. 6.

Experimentally the pure native-defect-controlled diffusion mode is hardly established since it requires that $\widetilde{C}_{AI^v} \approx 1$ holds. In general, dopant profiles in semiconductors exhibit a limited penetration depth. At the diffusion front the formation of A_s^- is not only controlled by native-point defects but also by the supply of the mobile dopant-defect pair. Hence, the native-defect-controlled mode of dopant diffusion becomes experimentally only visible in the shape of the dopant profile close to the surface.

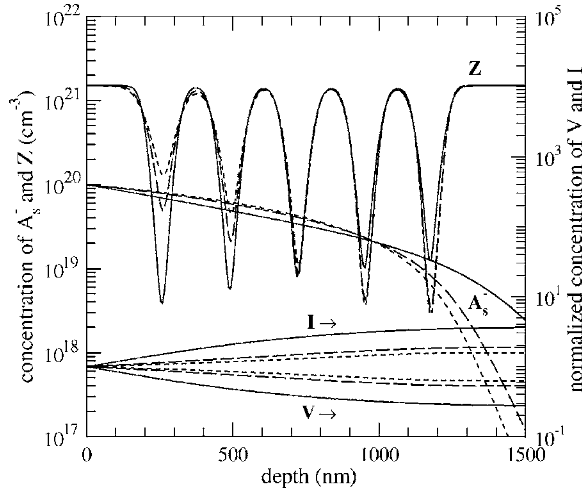

FIG. 7. Numerical simulations of A_s^-, V, and I profiles performed on the basis of reactions (2) and (6) for an intermediate mode of dopant diffusion (see text for details). The solid, long-dashed, and short-dashed lines represent calculations for I^0, I^+, and I^{2+}, respectively. The A_s^- profile becomes more box-shaped when the concentrations of V and I approach thermal equilibrium. The impact of doping on the equilibrium concentration of I^+ and I^{2+} leads to the enhanced self-diffusion in the region of extrinsic doping.

3. Intermediate mode of diffusion

The intermediate mode of dopant diffusion is obtained when the transport coefficients of the mobile dopant-defect pairs $C^{\mathrm{eq}}_{AV,AI}D_{AV,AI}$ or of the interstitial foreign atoms $C^{\mathrm{eq}}_{A_i}D_{A_i}$ are of the same order of magnitude as $C^{\mathrm{eq}}_{V,I}D_{V,I}$. Simulations for this mode are illustrated in Fig. 7. Again reactions (2) and (6) with various charge states of the native defects were considered. The figure demonstrates that the shape of the A_s^- profiles becomes more boxlike when the charge state of the self-interstitial changes from neutral to single and double positive. In the case that only neutral native defects exist, the depth-dependent broadening of the multilayer structure reflects the I supersaturation. In the case that positively charged self-interstitials exist, the impact of the Fermi level on the equilibrium concentration of I^+ leads to an increased self-diffusion in the region of high dopant concentrations. This increase is even more pronounced when the self-interstitials are doubly positively charged. With the increasing transport capacity of positively charged self-interstitials the supersaturation gets lower. This in turn affects the shape of the A_s^- profile. Finally, when $C_{V,I}$ approach the equilibrium value $C^{\mathrm{eq}}_{V,I}$, the dopant profile is fully box-shaped. Now the foreign-atom-controlled mode is established and the dopant profile has lost its sensitivity to the transport coefficients of the native-point defects.

Equation (75) takes into consideration that mobile dopant-defect pairs contribute to self-diffusion. This contribution can be significant for the native defect and intermediate mode of dopant diffusion when $D^*_{AV^j,AI^v} \gtrsim D^*_{V^k,I^u}$ holds. Figure 8 shows corresponding simulations of acceptor diffusion taking into account neutral AI^0 pairs with diffusion-correlation factors $f_{AI^0}=0.0$ (solid lines) and $f_{AI^0}=1.0$ (dashed lines). In the first case the pairs do not affect self-diffusion and in the later case they lead to an enhanced self-diffusion within the high concentration region of the dopant profile. This shows that dopant diffusion in the native-defect and intermediate-diffusion mode can help to differentiate between mobile interstitial foreign atoms and mobile dopant-defect pairs provided that the correlation factors for self-diffusion via pairs are not too small.

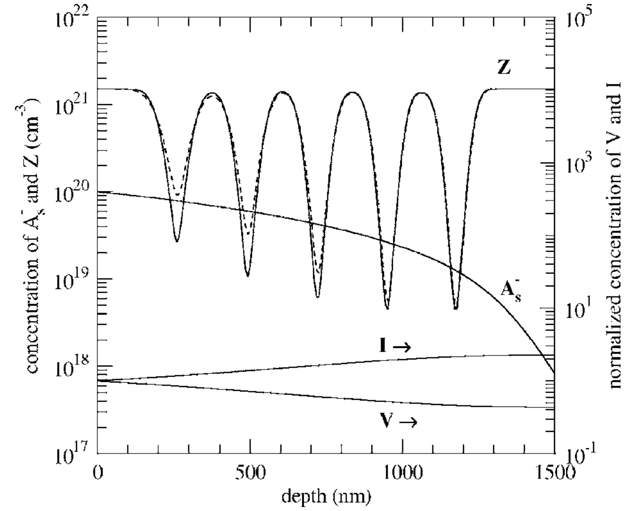

FIG. 8. Calculated acceptor A_s^- and self-atom-diffusion profiles and the corresponding normalized concentrations of V and I. The simulations were performed on the basis of reactions (2) and (6) for $D^*_{AI^0} \gtrsim D^*_{V^k,I^u}$ representing the intermediate and native-defect-controlled mode of dopant diffusion. Depending on the diffusion-correlation factor f_{AI^0} the self-diffusion can be affected by dopant-defect pairs (dashed line: $f_{AI^0}=1.0$) or not (solid line: $f_{AI^0}=0.0$). The model parameters used for the simulations are representative for B diffusion in Si (see Part II).

Another interesting aspect of the simultaneous self- and foreign-atom diffusion is whether such experiments can dis-

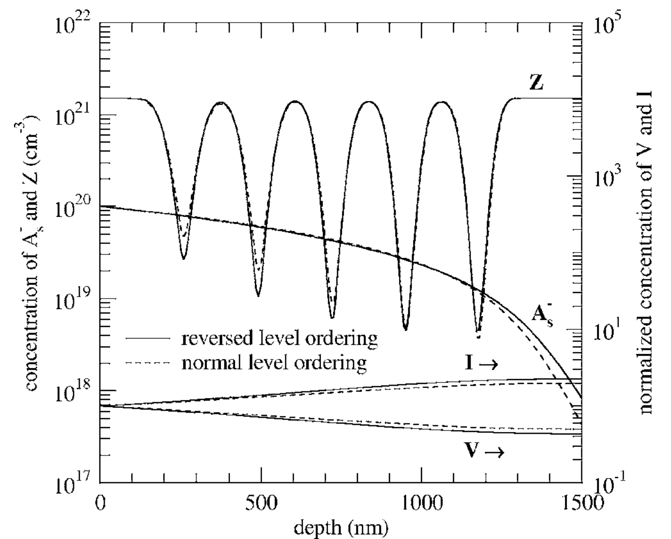

FIG. 9. Simulations of acceptor A_s^- and self-atom diffusion assuming a normal (dashed lines) and reversed (solid lines) level ordering for self-interstitials. The simulations are representative for B diffusion in Si (see Part II).

tinguish between normal and reversed level ordering of charged native defects. A reversed level ordering (negative-U center) was first predicted by theory[61] and subsequently proven by experiment[62,63] for the vacancy in silicon. According to the calculations of Car *et al.*,[4] the self-interstitial in silicon also behaves as a negative-U center. I^{2+} is the stable defect when the Fermi level E_f is in the lower half of the band gap whereas I^0 is preferred when E_f is in the upper half of the gap. I^+ is not a stable defect for any position of the Fermi level. Figure 9 illustrates simulations of the diffusion of an acceptor dopant via reactions (2) and (6) assuming a normal and reversed level ordering for self-interstitials. The model parameters used for the simulations are representative for modeling the diffusion of B in Si isotope structures (see Part II). Both the acceptor and self-atom profiles change when the level ordering of the self-interstitials is reversed. This demonstrates that diffusion studies can in principle provide evidence for the level ordering. However, the level ordering is hardly obtained when the analysis is concerned only with the diffusion of one dopant in an isotope structure because the small differences observed in Fig. 9 between the profiles can be compensated with other model parameters. But the demand to describe the diffusion of both acceptors and donors in semiconductor isotope structures with the same set of defect energy levels offers an additional constraint to determine the level ordering. In Part II the energy-level diagram of the native defects in Si is deduced from modeling the diffusion of B, As, and P in Si isotope multilayer structures and is compared with theoretical predictions for zero K. The simulations indicate a reversed level for Si self-interstitials also at high temperatures.

IV. CONCLUSION

Continuum theoretical calculations of atomic diffusion in semiconductors based on differential equations offer a robust and fast approach to describe experimental diffusion profiles. With this approach the impact of doping on self- and foreign-atom diffusion can be treated and therewith makes possible the description of the simultaneous diffusion of self- and foreign atoms in an isotopically controlled semiconductor. The simulations reveal the significance of the various model parameters on the shape of the dopant profile. In many cases the diffusion process is mainly determined by the transport coefficients $C_X^{\mathrm{eq}}D_X$ of the point defects X involved in the diffusion process. Basically two different diffusion modes, the foreign-atom- and native-defect-controlled modes, can be distinguished. These modes are characterized by specific relationships between the experimentally apparent effective diffusion coefficient of the dopant atom and the native-point defect that controls the formation of the substitutional dopant A_s^m. This relation is crucial for the understanding of dopant diffusion in semiconductors.

With the availability of isotopically controlled semiconductor multilayer structures, advanced diffusion studies can be performed whose analysis provides valuable information about the properties of native-point defects. The advantages of such studies become evident by simulations of the foreign-atom- and native-defect-controlled modes of dopant diffusion in an isotope multilayer structure. In the first case the charge states of native-point defects can be determined, which are not accessible when only the dopant profile is analyzed. In the latter case the diffusion profiles allow us to distinguish between the impact of doping and defect reactions on self-diffusion. Since one type of native defect is favored in the native-defect-controlled mode, the charge states and transport properties of this defect can be determined.

Due to the complexity of atomic-mass transport in semiconductors, which often proceeds via various mechanisms, it can be difficult to unambiguously identify the nature and charge states of point defects by means of diffusion experiments with one dopant element. A comprehensive study of dopant diffusion in semiconductors must consider the diffusion of *n*- and *p*-type dopants. Ideally, diffusion profiles of various dopants should be analyzed simultaneously in order to achieve a consistent picture on the diffusion mechanisms and properties of the point defects. The accomplishment of this challenging task was difficult due to the lack of appropriate semiconductor isotope heterostructures for diffusion experiments and the limited computer capacity. These restrictions no longer exist. Today, sophisticated diffusion studies can be performed with well-designed material heterostructures and the computing capacity of today's personal computers is sufficient to solve the complex diffusion equations within acceptable times. Although numerous diffusion studies have been performed with silicon, basic questions concerning the properties of self-interstitials and vacancies are still unsolved. In Part II the continuum theoretical approach described in this paper is applied to model the diffusion of B, P, and As in Si isotope multilayer structures.

ACKNOWLEDGMENT

This work was supported by the Deutsche Forschungsgemeinschaft under Contract No. Bra 1520/6-1.

*Electronic address: bracht@uni-muenster.de

[1] *Diffusion in Semiconductors and Non-Metallic Solids*, edited by D. L. Beke, Landolt-Börnstein, New Series, Group III, Vol. 33A (Springer, Berlin, 1998).

[2] *Impurities and Defects in Group IV Elements, IV-IV and III-V Compounds*, edited by M. Schulz, Landolt-Börnstein, New Series, Group III, Vol. 41A2, Part α (Springer, Berlin, 2002).

[3] *Impurities and Defects in Group IV Elements, IV-IV and III-V Compounds*, edited by M. Schulz, Landolt-Börnstein, New Series, Group III, Vol. 41A2, Part β (Springer, Berlin, 2003).

[4] R. Car, P. J. Kelly, A. Oshiyama, and S. T. Pantelides, Phys. Rev. Lett. **52**, 1814 (1984).

[5] Y. Bar-Yam and J. D. Joannopoulos, Phys. Rev. Lett. **52**, 1129 (1984).

[6] P. E. Blöchl, E. Smargiassi, R. Car, D. B. Laks, W. Andreoni, and S. T. Pantelides, Phys. Rev. Lett. **70**, 2435 (1993).

[7] S. J. Clark and G. J. Ackland, Phys. Rev. B **56**, 47 (1997).
[8] B. Sadigh, Th. J. Lenosky, S. K. Theiss, M.-J. Caturla, T. Diaz de la Rubia, and M. A. Foad, Phys. Rev. Lett. **83**, 4341 (1999).
[9] W.-K. Leung, R. J. Needs, G. Rajagopal, S. Itoh, and S. Ihara, Phys. Rev. Lett. **83**, 2351 (1999).
[10] W. Windl, M. M. Bunea, R. Stumpf, S. T. Dunham, and M. P. Masquelier, Phys. Rev. Lett. **83**, 4345 (1999).
[11] J.-W. Jeong and A. Oshiyama, Phys. Rev. B **64**, 235204 (2001).
[12] X.-Y. Liu, W. Windl, K. M. Beardmore, and M. P. Masquelier, Appl. Phys. Lett. **82**, 1839 (2003).
[13] O. K. Al-Mushadani and R. J. Needs, Phys. Rev. B **68**, 235205 (2003).
[14] G. M. Lopez and V. Fiorentini, Phys. Rev. B **69**, 155206 (2004).
[15] F. El-Mellouhi, N. Mousseau, and Pablo Ordejón, Phys. Rev. B **70**, 205202 (2004).
[16] E. G. Song, E. Kim, Y. H. Lee, and Y. G. Hwang, Phys. Rev. B **48**, 1486 (1993).
[17] M. Tang, L. Colombo, J. Zhu, and T. Diaz de la Rubia, Phys. Rev. B **55**, 14279 (1997).
[18] P. Alippi, L. Colombo, P. Ruggerone, A. Sieck, G. Seifert, and Th. Frauenheim, Phys. Rev. B **64**, 075207 (2001).
[19] A. Jääskeläinen, L. Colombo, and R. Nieminen, Phys. Rev. B **64**, 233203 (2001).
[20] H. R. Schober, Phys. Rev. B **39**, 13013 (1989).
[21] D. Maroudas and R. A. Brown, Appl. Phys. Lett. **62**, 172 (1993).
[22] D. Maroudas and R. A. Brown, Phys. Rev. B **47**, 15562 (1993).
[23] M. Posselt, F. Gao, and D. Zwicker, Phys. Rev. B **71**, 245202 (2005).
[24] S. T. Dunham and Can Dong Wu, J. Appl. Phys. **78**, 2362 (1995).
[25] W. Frank, U. Gösele, H. Mehrer, and A. Seeger, in *Diffusion in Crystalline Solids*, edited by G. E. Murch and A. S. Nowick (Academic Press, New York, 1984).
[26] U. M. Gösele, Annu. Rev. Mater. Sci. **18**, 257 (1988).
[27] M. D. Giles, IEEE Trans. Comput.-Aided Des. **8**, 460 (1989).
[28] P. M. Fahey, P. B. Griffin, and J. D. Plummer, Rev. Mod. Phys. **61**, 289 (1989).
[29] U. Gösele and T. Y. Tan, in *Electronic Structure and Properties of Semiconductors*, edited by W. Schröter (VCH, Weinheim, 1991), p. 197.
[30] M. D. Giles, Appl. Phys. Lett. **58**, 2399 (1991).
[31] S. Yu, T. Y. Tan, and U. Gösele, J. Appl. Phys. **70**, 4827 (1991).
[32] H. Bracht, N. A. Stolwijk, and H. Mehrer, Phys. Rev. B **43**, 14465 (1991).
[33] N. E. B. Cowern, G. F. A. van de Walle, D. J. Gravesteijn, and C. J Vriezema, Phys. Rev. Lett. **67**, 212 (1991).
[34] H. Bracht, N. A. Stolwijk, and H. Mehrer, Phys. Rev. B **52**, 16542 (1995).
[35] M. Uematsu, J. Appl. Phys. **82**, 2228 (1997).
[36] A. Ural, P. B. Griffin, and J. D. Plummer, Phys. Rev. B **65**, 134303 (2002).
[37] A. M. Saad and O. I. Velichko, Mater. Sci. Semicond. Process. **7**, 27 (2004).
[38] H. Bracht and S. Brotzmann, Phys. Rev. B **71**, 115216 (2005).
[39] W. Shockley and J. L. Moll, Phys. Rev. **119**, 1480 (1960).
[40] $D_{A_s^m}$ in Eq. (27) equals the diffusivity $D_{A_s^m}^{\mathrm{ex}}$ of the substitutionally dissolved foreign atom via direct exchange.
[41] S. Mizuo and H. Higuchi, Jpn. J. Appl. Phys. **20**, 739 (1981).
[42] S. Mizuo and H. Higuchi, Jpn. J. Appl. Phys., Part 1 **21**, 56 (1982).
[43] S. Mizuo, T. Kusaka, A. Shintani, M. Nanba, and H. Higuchi, J. Appl. Phys. **54**, 3860 (1983).
[44] S. Matsumoto, Y. Ishikawa, and T. Niimi, J. Appl. Phys. **54**, 5049 (1983).
[45] Y. Ishikawa, M. Tomisato, H. Honma, S. Matsumoto, and T. Niimi, J. Electrochem. Soc. **130**, 2109 (1983).
[46] P. Fahey, G. Barbuscia, M. Moslehi, and R. W. Dutton, Appl. Phys. Lett. **46**, 784 (1985).
[47] M. Miyake, J. Appl. Phys. **57**, 1861 (1985).
[48] Y. Ishikawa, I. Nakamichi, S. Matsumoto, and T. Niimi, Jpn. J. Appl. Phys., Part 1 **26**, 1602 (1987).
[49] H.-J. Gossmann, T. E. Haynes, P. A. Stolk, D. C. Jacobson, G. H. Gilmer, J. M. Poate, H. S. Luftman, T. K. Mogi, and M. O. Thompson, Appl. Phys. Lett. **71**, 3862 (1997).
[50] I. D. Sharp, H. A. Bracht, H. H. Silvestri, S. P. Nicols, J. W. Beeman, J. Hansen, A. Nylandsted Larsen, and E. E. Haller, in *Defect and Impurity Engineered Semiconductor and Devices III*, edited by S. Ashok, J. Chevallier, N. M. Johnson, B. L. Sopori, and H. Okushi, MRS Symposia Proceedings No. 719 (Materials Research Society, Pittsburgh, 2002), p. F13.11.
[51] H. H. Silvestri, I. D. Sharp, H. A. Bracht, S. P. Nicols, J. W. Beeman, J. Hansen, A. Nylandsted Larsen, and E. E. Haller, in *Defect and Impurity Engineered Semiconductor and Devices III*, edited by S. Ashok, J. Chevallier, N. M. Johnson, B. L. Sopori, and H. Okushi, MRS Symposia Proceedings No. 719 (Materials Research Society, Pittsburgh, 2002), p. F13.10.
[52] H. Bracht, H. H. Silvestri, I. D. Sharp, S. P. Nicols, J. W. Beeman, J. L. Hansen, A. Nylandsted Larsen, and E. E. Haller, Inst. Phys. Conf. Ser. **171**, C3.8.76 (2003).
[53] H. H. Silvestri, H. Bracht, I. D. Sharp, J. Lundsgaard Hansen, A. Nylandsted Larsen, and E. E. Haller, in *Silicon Front-End Junction Formation Physics and Technology*, edited by P. Pichler, A. Claverie, R. Lindsay, M. Orlowski, and W. WindlMRS Symposia Proceedings No. 810 (Materials Research Society, Pittsburgh, 2004), p. C3.3.
[54] H. Bracht, H. H. Silvestri, and E. E. Haller, Solid State Commun. **133**, 727 (2005).
[55] H. Bracht, Physica B **376–377**, 11 (2006).
[56] These relationships follow from Eq. (65) and $n_{\mathrm{in}}/p^{\mathrm{eq}}=\exp\{(E_f-E_f^{\mathrm{in}})/k_BT\}$.
[57] W. Jüngling, P. Pichler, S. Selberherr, E. Guerrero, and H. W. Pötzl, IEEE Trans. Electron Devices **32**, 156 (1985).
[58] The settings are, in particular, realistic with regard to dopant diffusion in Si (see Part II) where the solubilities of dopants like B, P, and As are in the range of 10^{20} cm^{-3} at, e.g., 1000 °C and five or even more orders of magnitude higher than the thermal equilibrium concentrations of vacancies and self-interstitials.
[59] K. Sunder, Diploma thesis, University of Muenster, 2006.
[60] The interstitialcy mechanism (2) possesses a reaction scheme equal to the vacancy mechanism (1).
[61] G. A. Baraff, E. O. Kane, and M. Schlüter, Phys. Rev. Lett. **43**, 956 (1979).
[62] G. D. Watkins, in *Festkörperprobleme (Advances in Solid State Physics)*, edited by P. Grosse (Viewig, Braunschweig, 1984), Vol. XXIV, p. 163.
[63] G. D. Watkins, in *Defects and Diffusion in Silicon Processing*, edited by T. D. de la Rubia, S. Coffa, P. A. Stolk, and C. S. Rafferty, MRS Symposia Proceedings No. 469 (Materials Research Society, Pittsburgh, 1997), p. 139.